

Forecasting stock market crashes through entropy-based proper measures of connectedness

Mishel Qyrana*

November 9, 2024

Abstract

We propose a class of systemic risk indicators based on the entropy measures introduced by Rényi. We begin by demonstrating how well-known entropy measures and their properties can be derived from Rényi's definition. Once the systemic risk measure is defined, we show that it qualifies as a proper measure of connectedness, highlighting its consistent and unifying behavior compared to other approaches recently proposed in the literature. This is followed by an in-depth empirical analysis of the predictive capabilities of the indicator with respect to stock market crashes. The analyses are conducted on two datasets, reconfigured into three possible combinations and for two potential daily forecasting horizons. The performance of the proposed indicator is compared with that of similar indicators suggested in the literature. According to the majority of metrics, the indicator outperforms across all tests against competing indicators.

Keywords: Systemic risk, Credit Market Risk, Connectedness, Financial markets, Portfolio management, Financial Machine Learning

JEL Classification: C45, C51, C52, C53, C61, C63, C67

1 Introduction and literature review

Systemic crashes are a defining feature of financial crises, characterized by the collapse of large segments of the financial system, leading to widespread economic disruption. The 2007-2008 subprime crisis, in particular, renewed interest in the accurate measurement of risk among both policymakers and academics. This interest is rooted in the need for early warning systems that can predict various types of financial crises, such as banking, currency, or debt crises, allowing authorities enough time to implement appropriate interventions (e.g., Alessi and Detken, 2011). However, the models and measures that existed prior to the crisis largely failed to provide adequate warnings, revealing their static

*Quantitative Researcher at Generali Asset Management.
Email:
mishel.qyrana@generali-invest.com

nature and dependence on changes in exogenous macroeconomic variables, which proved insufficient to explain the dynamics of systemic risk (Rose and Spiegel, 2012).

Since the late 1970s, efforts to model systemic crashes have taken various forms. Early research was prompted by the surge of currency crises, leading to the development of crisis indicators (Bilson, 1979) and theoretical models (Krugman, 1979). Subsequent approaches, such as those by Kaminsky (1999) and Frankel and Saravelos (2010), utilized variable selection criteria to create single and multivariate models for estimating the probability of future crises. Despite their contributions, these models often fell short of anticipating major systemic events due to their limitations in capturing the intricate dynamics of interconnected financial systems.

In this regard, warning indicators based on endogenous analyses have begun to flourish in the literature. An essential aspect of systemic crashes is their strong link to the presence of market bubbles, which often precede crises. Not surprisingly, some of the first notable contributions have come from Econophysics, specifically modeling bubbles and the crashes associated with them. Sornette et al. (1996), Sornette and Johansen (1997), and Johansen et al. (2000) argued that prior to market crashes, the mean function of a stock index price series tends to follow a power law with log-periodic oscillations, culminating in a critical point marking the onset of the crash. The Johansen-Ledoit-Sornette (JLS) model further provides insight by micro-founding the price behaviors on two types of market participants: rational traders and noise traders who engage in irrational herding. The JLS model, inspired by statistical physics, describes market dynamics as networks of traders whose decisions are influenced by others' actions, akin to the Ising model for ferromagnetism (Goldenfeld, 1992). These interactions can lead to self-similar behavior among groups of traders, potentially pushing markets into a bubble—a state of order, distinct from the more disordered state of normal market conditions.

The underlying idea of trader networks and the derived herding behavior has a natural connection with the concept of connectedness. High market connectedness plays a crucial role in the formation and burst of bubbles, acting as a major driver of systemic crashes. When financial assets exhibit high connectedness, a shock to one component quickly spreads across the system, often leading to cascading failures and reducing diversification opportunities. The concept of connectedness was first introduced by Diebold and Yilmaz (2009), who aimed to quantify the degree of interrelation and interdependence among components of a financial system. Since then, many studies have sought to measure the connectedness of financial systems, including those by Andersen et al. (2010), Baruník et al. (2016), Diebold and Yilmaz (2014), Demirer et al. (2018), and Zhang and Broadstock (2018). These measures serve to summarize the complex web of interdependencies among financial agents, such as firms or assets, into a single index. In economic and financial contexts, a higher level of connectedness intuitively implies increased systemic risk. For instance, high connectedness among asset returns means a lack of effective diversification opportunities, amplifying the potential impact of shocks.

Various attempts have been made to develop measures of connectedness to better understand systemic risk. These include approaches related to market risk (e.g., return connectedness and market diversification by Belsey et al., 1980), credit risk (e.g., default connectedness by Merton, 2014), and systemic risk in general (e.g., Billio et al., 2012; Figini et al., 2018; Acemoglu et al., 2015; Acharya et al., 2012). Diebold and Yilmaz (2012) highlighted that high financial interconnectedness often leads to significant volatility spillovers both within and across markets. This heightened level of connectedness exacerbates systemic risks during periods of crisis, as volatility and correlated returns converge, reducing diversification opportunities.

The literature on connectedness typically employs correlation-based measures, despite their limitations in capturing the complexity of financial interactions (Diebold and Yilmaz, 2014). Correlation provides a useful yet incomplete view of the multidimensional nature of connectedness, which encompasses not only linear relationships but also higher-order dynamics.

Different from approaches based on the largest eigenvalues and absorption ratio like in Billio et al. (2012), Figini et al. (2018) explored the behavior of the smallest eigenvalues of the covariance matrix, particularly those close to zero, as indicators of diversification opportunities at risk. This work introduced the Market Rank Indicator, which belongs to a broader family of indicators based on Chisini's classical definition of mean (Maggi et al., 2022). In the same paper for the first time it was axiomatically defined the concept of *proper measure of connectedness*, also empirically showing that systemic risk indicators adhering to this formal definition generally exhibit stronger predictive power than those that do not.

Building on these ideas, Qyrana et al. (2024) proposed the Adjusted Diversification Loss Index, which directly maps the number of dimensions at risk onto the correlation matrix. This index captures the number of diversification opportunities at risk within the market by counting the number of eigenvalues below the adjusted threshold predicted by the Marchenko-Pastur distribution. To achieve this, the authors used a correlation matrix computed from latent factors learned by an autoencoder, providing a more refined assessment of market interconnectedness.

In this work, we aim to address the issue of how many and which eigenvalues to consider in order to understand the loss of diversification opportunities in the equity market and the onset of systemic risk situations. This is done by applying systemic risk indicators given by the negative of Rényi entropy measures calculated on the eigenvalues of appropriately rescaled covariance or correlation matrices. This approach frees us from the choice of significant eigenvalues for identifying systemic risk collapses, capturing dynamics related to both the behavior of the largest eigenvalues and those of smaller magnitude, as well as their relative magnitudes.

Rényi entropy is a versatile family of entropy measures that extends the concept of Shannon entropy and more generally provides a unified framework for studying different entropy

measures by simply varying α (Rényi, 1961).

In information theory, Rényi entropy has been applied to analyze coding efficiency and redundancy, as well as to generalize channel capacity definitions (Cover et al., 2006). In statistical mechanics, it aids in studying systems with non-extensive properties. Quantum information theory benefits from Rényi entropy through its use in quantifying quantum correlations and studying entanglement, Müller-Lennert et al. (2013). In ecology and biodiversity, Rényi entropy helps measure species diversity by considering both richness and evenness. Additionally, in machine learning, it is used for feature selection and anomaly detection, enhancing the ability to identify informative features and detect deviations from expected entropy levels.

Collision entropy, a specific case of Rényi entropy when $\alpha = 2$, measures the likelihood of identical outcomes in repeated sampling. This measure is particularly relevant in cryptography for analyzing hash collisions and assessing the strength of cryptographic keys. It also finds applications in data privacy, randomness testing, and signal processing (Van Erven et al, 2014).

Caraiani (2014) employs a correlation-based approach to analyze financial data from the US stock market, using both daily and monthly observations from the Dow Jones. The study computes entropy based on the singular value decomposition of the correlation matrix for the components of the Dow Jones Industrial Index. By utilizing a moving window, time-varying measures of entropy are derived for both daily and monthly data. The findings indicate that entropy has a predictive ability regarding stock market dynamics, as evidenced by Granger causality tests.

Espinosa et al. (2022) investigate the impact of the Covid-19 outbreak on crude oil market efficiency using a singular value decomposition (SVD) entropy approach. The study contrasts results against random patterns using iso-distributional surrogate data tests and assesses nonlinearities through phase randomization based on Fourier transform. The results show that the crude oil market was mostly informationally efficient with sporadic deviations pre-Covid-19, while the pandemic period exhibited significant deviations from efficiency, especially in the initial months, accompanied by a reduction in nonlinear components. The study also examines trading volume dynamics, revealing that market activity is not fully random and exhibits significant deviations from randomness when the crude oil market is efficient.

Gu (2017) performs a multiscale entropy analysis on the Dow Jones Industrial Average Index using Shannon entropy. The study demonstrates that the stock index exhibits multi-scale entropy characteristics caused by market noise. The entropy is shown to have significant predictive ability for the stock index in both long-term and short-term, with empirical results verifying the presence of noise in the market and its impact on stock prices. This has important implications for market participants, such as noise traders.

Civitarese (2016) addresses the use of simple systemic risk measures to assess portfolio risk characteristics. The study uses examples based on raw and partial correlations, eigenvalue

decomposition of the covariance matrix, and eigenvalue entropy. A Granger-causation analysis reveals that these measures are not always good indicators of risk in the S&P 500 and VIX indices. The selected measures do not consistently Granger-cause the VIX index, indicating that they are not always suitable as volatility risk indicators. However, their results regarding returns are consistent with previous works. The study concludes that symmetric measures based on eigenvalue decomposition of correlation matrices are not useful as measures of “correlation” risk.

Koushki (2023) employs Pearson correlation and a multiscale generalized Shannon-based entropy to trace the transition and type of inherent mutual information and correlation structures. It finds that mutual information between emerging markets entails higher sensitivity, with emerging markets demonstrating the highest uncertainty among investigated markets. The study also shows that emerging markets are becoming more efficient over time, with long-term lag and synchronous phases between developed and emerging markets. The Covid-19 pandemic period is highlighted, showing higher uncertainty and overreaction in emerging markets.

Caraiani (2018) proposes a methodology to study the comovement between the entropy of different financial markets using singular value decomposition of stock market indices from developed economies (France, Germany, the United Kingdom, and the United States). The study examines how a shock in the entropy in the United States affects the entropy in other financial markets and models the entropy using a dynamic factor model to derive a common factor behind entropy movements in these markets.

Jiang (2016) generalizes the method of traditional singular value decomposition entropy by incorporating orders of Rényi entropy. The study analyzes the predictive power of the entropy based on the trajectory matrix using data from the Shanghai Composite Index (SCI) and the Dow Jones Index (DJI) in both static and dynamic tests, finding that noise and errors affect SCI more frequently than DJI.

Lupu (2020) investigates the dynamics of systemic risk of European companies using an approach that merges paradigmatic risk measures such as Marginal Expected Shortfall, CoVaR, and Delta CoVaR with a Bayesian entropy estimation method. The study aims to highlight potential spillover effects of the entropy indicator for systemic risk measures computed on the 24 sectors that compose the STOXX 600 index. The results show that several sectors, including Capital Goods, Banks, Diversified Financials, Insurance, and Real Estate, have a high proclivity for generating spillovers.

Lupu (2022) focuses on ensuring financial stability, a primary objective of authorities supervising financial markets. The paper documents the dependence of extreme systemic risk situations on market actions in preceding time intervals. The study detects anomalies (jumps) in the dynamics of CoVaR measures for the most liquid banks in European markets and measures the Shannon entropy of the power spectral density in samples leading to these events. Several logistic regressions are employed to document the capacity of entropy to explain the realization of these anomalies.

This paper is organized as follows: in the first section, we state the definition of Rényi entropy measure, its properties, and show how Shannon entropy and collision entropy are obtained as special cases of this; in the second section, we demonstrate that Rényi entropy measures calculated on appropriately rescaled eigenvalues of a covariance matrix are proper measures of connectedness; in the third section, we show the connection that links the Market Rank Indicator and, more generally, indicators based on Chisini means, the Adjusted Diversification Loss Index, and measures based on the definition of Rényi entropy; the article concludes with an empirical analysis section aimed at evaluating the predictive power of the proposed indicators from different perspectives, using twenty years of data related to the S&P 500 and the MSCI World Index.

2 The Rényi entropy measures: general definition and particular cases

Rényi entropy is a family of entropy measures that generalizes the Shannon entropy. For a discrete probability distribution $P = \{p_i\}$ and a real parameter $\alpha \geq 0$ (with $\alpha \neq 1$), the Rényi entropy of order α is defined as:

$$H_\alpha(P) = \frac{1}{1-\alpha} \log \left(\sum_i p_i^\alpha \right). \quad (1)$$

So defined, Rényi entropies have some basic properties:

- **Non-Negativity:** $H_\alpha(P) \geq 0$.
- **Additivity for Independent Distributions:** For independent distributions P and Q :

$$H_\alpha(P \times Q) = H_\alpha(P) + H_\alpha(Q).$$

- **Monotonicity:** Rényi entropy is non-increasing with respect to α :

$$\text{If } \alpha < \beta, \quad H_\alpha(P) \geq H_\beta(P).$$

By varying α different well-known entropy measures can be obtained.

Proposition 2.1. *When α tends to 1, the Rényi entropy converges to the Shannon entropy:*

$$\lim_{\alpha \rightarrow 1} H_\alpha(P) = H(P) = - \sum_i p_i \log p_i. \quad (2)$$

Proof. To show this result we want then to compute the limit:

$$\lim_{\alpha \rightarrow 1} H_\alpha(P) = \lim_{\alpha \rightarrow 1} \frac{1}{1-\alpha} \log \left(\sum_i p_i^\alpha \right).$$

First we can expand $\sum_i p_i^\alpha$ around $\alpha = 1$. To ease things, we start from a little trick:

$$p_i^\alpha = p_i^{1+(\alpha-1)} = p_i \cdot p_i^{\alpha-1} = p_i \cdot e^{(\alpha-1) \log p_i}.$$

Since $\alpha - 1$ is small, we expand $e^{(\alpha-1) \log p_i}$:

$$e^{(\alpha-1) \log p_i} = 1 + (\alpha - 1) \log p_i + \frac{1}{2}(\alpha - 1)^2 (\log p_i)^2 + \dots$$

Thus,

$$p_i^\alpha = p_i \left[1 + (\alpha - 1) \log p_i + \frac{1}{2}(\alpha - 1)^2 (\log p_i)^2 + \dots \right].$$

Summing over i we obtain:

$$\sum_i p_i^\alpha = \sum_i p_i \left[1 + (\alpha - 1) \log p_i + \frac{1}{2}(\alpha - 1)^2 (\log p_i)^2 + \dots \right].$$

Now, by exploiting the fact that by construction the sum of p_i -s is by definition equal to one and taking the multiplicative constants out of the sums, we can simplify as:

$$\sum_i p_i^\alpha = 1 + (\alpha - 1) \sum_i p_i \log p_i + \frac{1}{2}(\alpha - 1)^2 \sum_i p_i (\log p_i)^2 + \dots$$

Then taking the logarithm we have:

$$\log \left(\sum_i p_i^\alpha \right) = \log \left[1 + (\alpha - 1) \sum_i p_i \log p_i + \dots \right].$$

By expanding it again around 0 using the fact that for $\alpha \rightarrow 1$ then $\alpha - 1 \rightarrow 0$, the logarithm expanded in Taylor series around $x = 0$ will be:

$$\log(1 + x) = x - \frac{x^2}{2} + \frac{x^3}{3} - \dots$$

So in our case of interest we obtain:

$$\log \left(\sum_i p_i^\alpha \right) = (\alpha - 1) \sum_i p_i \log p_i - \frac{1}{2}(\alpha - 1)^2 \left(\sum_i p_i \log p_i \right)^2 + \dots$$

Now we compute $H_\alpha(P)$:

$$H_\alpha(P) = -\frac{1}{\alpha - 1} \left[(\alpha - 1) \sum_i p_i \log p_i - \frac{1}{2}(\alpha - 1)^2 \left(\sum_i p_i \log p_i \right)^2 + \dots \right].$$

Which can be simplified as:

$$H_\alpha(P) = - \left[\sum_i p_i \log p_i - \frac{\alpha - 1}{2} \left(\sum_i p_i \log p_i \right)^2 + \dots \right].$$

Finally, we take the limit as $\alpha \rightarrow 1$:

$$\lim_{\alpha \rightarrow 1} H_\alpha(P) = - \sum_i p_i \log p_i = H(P).$$

□

That said, we obtain the so called collision entropy simply as the Rényi entropy when $\alpha = 2$:

$$H_2(P) = -\log \left(\sum_i p_i^2 \right). \quad (3)$$

so that it is the negative logarithm of the *collision probability*, i.e., of the probability that two independent random variables, both described by the same probability distribution, will take the same value. For this reason, it can be interpreted as distribution concentration measure: a higher collision probability (lower collision entropy) indicates that the distribution is more concentrated on certain outcomes.

Other well-known entropy measures which can be obtained from the general Rényi definition are the Hartley Entropy ($\alpha = 0$):

$$H_0(P) = \log N,$$

where N is the number of non-zero probabilities, as well as the Min-Entropy, obtained with $\alpha \rightarrow \infty$:

$$H_\infty(P) = -\log \left(\max_i p_i \right).$$

3 A Rényi entropy based proper measure of connectedness

Let $A \in \mathcal{M}_{T \times n}(\mathbb{R})$ be a full-ranked random matrix where $T > n$, with $\mathcal{M}_{T \times n}(\mathbb{R})$ denoting the set of real matrices of full rank, n representing the number of random variables, and T the number of observations. Let $\Xi(A) \in \mathcal{M}_{n \times n}(\mathbb{R})$ denote the empirical covariance matrix of A , with eigenvalues $0 \leq \lambda_1 \leq \dots \leq \lambda_n$. Finally let $P = \{p_i\}$ with $p_i = \frac{\lambda_i}{\sum_{j=1}^n \lambda_j}$ and a real parameter $\alpha \geq 0$ (with $\alpha \neq 1$).

Definition 3.1. The entropy-based measure of connectedness (EC) $\mu(A)$ is defined through the Rényi entropy of order α as:

$$\mu(A) = \frac{1}{1 + H_\alpha(P)} = \frac{1}{1 + \frac{1}{1-\alpha} \log (\sum_i p_i^\alpha)}. \quad (4)$$

Now we recall the definition of proper measure of connectedness, as stated in Maggi et al. (2020).

Definition 3.2. A function $\mu : \mathcal{M}_{T \times n}(\mathbb{R}) \rightarrow \mathbb{R}$ is a proper measure of connectedness if it satisfies the following properties:

1. $\mu(A) \geq 0$ for all $A \in \mathcal{M}_{T \times n}(\mathbb{R})$;
2. $\mu(A)$ is invariant under permutation of the columns of A for all $A \in \mathcal{M}_{T \times n}(\mathbb{R})$;
3. $\mu(A) > \mu(B)$ if and only if $\mu(\beta A) > \mu(\beta B)$ for $\beta > 0$ and for all $A, B \in \mathcal{M}_{T \times n}(\mathbb{R})$;

4. For $a_1, a_2, a_3 \in \mathcal{M}_{T \times 1}(\mathbb{R})$ such that $\|a_2\| = \|a_3\|$ and $|\langle \mathbf{1}, a_2 \rangle| = |\langle \mathbf{1}, a_3 \rangle| = 0$, if $|\rho(a_1, a_2)| \geq |\rho(a_1, a_3)|$, then $\mu(A_{12}) \geq \mu(A_{13})$, where $A_{1j} = (a_1 \mid a_j)$ for $j \in \{2, 3\}$.

Proposition 3.3. *The EC is a proper measure of connectedness.*

Proof. We proceed by verifying the four properties.

1. Property 1 is naturally satisfied from the properties of the Rényi entropy measures.
2. Property 2 is satisfied because the eigenvalues on which the probabilities are based are invariant with respect to similarity transformations.
3. As for Property 3, we have that scaling A by a positive scalar β , scales all entries of A by β . This is reflected in the covariance matrix $\Xi(\beta A)$ through a scaling by β^2 :

$$\Xi(\beta A)' = \text{Cov}(\beta A) = \beta^2 \Xi(A).$$

The eigenvalues λ_i scale by β^2 :

$$\lambda'_i = \beta^2 \lambda_i.$$

The sum of the eigenvalues scales by β^2 :

$$\sum_{i=1}^n \lambda'_i = \beta^2 \sum_{i=1}^n \lambda_i.$$

The normalized eigenvalues p_i remain unchanged:

$$p'_i = \frac{\lambda'_i}{\sum_{j=1}^n \lambda'_j} = \frac{\beta^2 \lambda_i}{\beta^2 \sum_{j=1}^n \lambda_j} = p_i.$$

Therefore, $\mu(\beta A) = \mu(A)$, and similarly for $\mu(\beta B) = \mu(B)$. So we conclude that since $\mu(\beta A) = \mu(A)$ and $\mu(\beta B) = \mu(B)$:

$$\mu(A) > \mu(B) \implies \mu(\beta A) = \mu(\beta B) > \mu(B) = \mu(\beta B).$$

4. As for property 4, let $a_1, a_2, a_3 \in \mathcal{M}_{T \times 1}(\mathbb{R})$ such that $\|a_2\| = \|a_3\|$ and $|\langle \mathbf{1}, a_2 \rangle| = |\langle \mathbf{1}, a_3 \rangle| = 0$ and $A_{1j} = (a_1 \mid a_j)$ for $j \in \{2, 3\}$. Let the variances of respectively a_1, a_2, a_3 be $\sigma_1^2, \sigma_2^2, \sigma_3^2$.

$$\Xi(A_{12}) = \begin{pmatrix} \sigma_1^2 & \sigma_1 \sigma_2 \rho_{12} \\ \sigma_1 \sigma_2 \rho_{12} & \sigma_2^2 \end{pmatrix},$$

where $\rho_{12} = \rho(a_1, a_2)$. For A_{13} we have:

$$\Xi(A_{13}) = \begin{pmatrix} \sigma_1^2 & \sigma_1 \sigma_3 \rho_{13} \\ \sigma_1 \sigma_3 \rho_{13} & \sigma_3^2 \end{pmatrix},$$

where $\rho_{13} = \rho(a_1, a_3)$. The we know that for a 2×2 symmetric matrix:

$$\Xi(A_{12}) = \begin{pmatrix} \sigma_1^2 & \sigma_1\sigma_2\rho \\ \sigma_1\sigma_2\rho & \sigma_2^2 \end{pmatrix},$$

the eigenvalues λ_1 and λ_2 are given by:

$$\lambda_{1,2} = \frac{\sigma_1^2 + \sigma_2^2 \pm \sqrt{(\sigma_1^2 - \sigma_2^2)^2 + 4\sigma_1^2\sigma_2^2\rho^2}}{2}.$$

Let $D = \sqrt{(\sigma_1^2 - \sigma_2^2)^2 + 4\sigma_1^2\sigma_2^2\rho^2}$. Then:

$$\lambda_1 = \frac{\sigma_1^2 + \sigma_2^2 + D}{2}, \quad \lambda_2 = \frac{\sigma_1^2 + \sigma_2^2 - D}{2}.$$

The total variance hence is:

$$\text{tr}(\Xi(A_{12})) = \sigma_1^2 + \sigma_2^2.$$

The probabilities are then:

$$p_1 = \frac{\lambda_1}{\sigma_1^2 + \sigma_2^2} = \frac{1}{2} \left(1 + \frac{D}{\sigma_1^2 + \sigma_2^2} \right),$$

$$p_2 = \frac{\lambda_2}{\sigma_1^2 + \sigma_2^2} = \frac{1}{2} \left(1 - \frac{D}{\sigma_1^2 + \sigma_2^2} \right).$$

Now we are interested in analyzing the dependence of D on $|\rho|$. Let:

$$D = \sqrt{(\sigma_1^2 - \sigma_2^2)^2 + 4\sigma_1^2\sigma_2^2\rho^2},$$

then differentiating D with respect to $|\rho|$ we get:

$$\frac{dD}{d|\rho|} = \frac{4\sigma_1^2\sigma_2^2|\rho|}{D} > 0.$$

Thus, D is an increasing function of $|\rho|$. Now let's compute the Rényi entropy measure for our case. Let:

$$S \equiv p_1^\alpha + p_2^\alpha.$$

Then:

$$H_\alpha(P) = \frac{1}{1-\alpha} \log S.$$

Then we take the derivative of $H_\alpha(P)$ with Respect to $|\rho|$. We start from derivative of S :

$$\frac{dS}{d|\rho|} = \alpha \left[p_1^{\alpha-1} \frac{dp_1}{d|\rho|} + p_2^{\alpha-1} \frac{dp_2}{d|\rho|} \right].$$

In particular, calculating the derivatives $\frac{dp_1}{d|\rho|}$ and $\frac{dp_2}{d|\rho|}$ gives:

$$\frac{dp_1}{d|\rho|} = \frac{1}{2} \cdot \frac{d}{d|\rho|} \left(\frac{D}{\sigma_1^2 + \sigma_2^2} \right) = \frac{1}{2(\sigma_1^2 + \sigma_2^2)} \cdot \frac{dD}{d|\rho|},$$

$$\frac{dp_2}{d|\rho|} = -\frac{1}{2} \cdot \frac{d}{d|\rho|} \left(\frac{D}{\sigma_1^2 + \sigma_2^2} \right) = -\frac{1}{2(\sigma_1^2 + \sigma_2^2)} \cdot \frac{dD}{d|\rho|}.$$

If we plug the result back into $\frac{dS}{d|\rho|}$ then we have:

$$\frac{dS}{d|\rho|} = \alpha \left[p_1^{\alpha-1} \left(\frac{1}{2(\sigma_1^2 + \sigma_2^2)} \cdot \frac{dD}{d|\rho|} \right) - p_2^{\alpha-1} \left(\frac{1}{2(\sigma_1^2 + \sigma_2^2)} \cdot \frac{dD}{d|\rho|} \right) \right].$$

The collecting $\frac{\alpha}{2(\sigma_1^2 + \sigma_2^2)} \cdot \frac{dD}{d|\rho|}$ we can rewrite:

$$\frac{dS}{d|\rho|} = \frac{\alpha}{2(\sigma_1^2 + \sigma_2^2)} \cdot \frac{dD}{d|\rho|} (p_1^{\alpha-1} - p_2^{\alpha-1}).$$

Since $\frac{dD}{d|\rho|} > 0$, the sign of $\frac{dS}{d|\rho|}$ depends on $p_1^{\alpha-1} - p_2^{\alpha-1}$. About this, we first note that $p_1 > p_2$ because $D > 0$. At this point we have two possible cases to address, related to the value of α . With $0 \leq \alpha < 1$ and then $\alpha - 1 < 0$, given that $p_1 > p_2$ and $\alpha - 1 < 0$, it follows that $p_1^{\alpha-1} < p_2^{\alpha-1}$. Therefore, $p_1^{\alpha-1} - p_2^{\alpha-1} < 0$. From this we obtain that the derivative of S with respect to d is structured as:

$$\frac{dS}{d|\rho|} = \text{Positive constant} \times (\text{Negative quantity}) = \text{Negative}.$$

Thus, $\frac{dS}{d|\rho|} < 0$ when $\alpha < 1$. Now we can complete the reasoning by taking the derivative of $H_\alpha(P)$ with Respect to $|\rho|$:

$$\frac{dH}{d|\rho|} = \frac{1}{1-\alpha} \cdot \frac{1}{S} \cdot \frac{dS}{d|\rho|}.$$

Since $\frac{dS}{d|\rho|} < 0$ and $S > 0$, the sign of $\frac{dH}{d|\rho|}$ depends on $\frac{1}{1-\alpha}$, and for $0 \leq \alpha < 1$, obviously $1 - \alpha > 0 \implies \frac{1}{1-\alpha} > 0$. Therefore, $\frac{dH}{d|\rho|} < 0$.

$H_\alpha(P)$ decreases as $|\rho|$ increases when $0 \leq \alpha < 1$, regardless of the variances of the variables. Therefore, if $|\rho_{12}| \geq |\rho_{13}|$, then our entropy-based measure of connectedness acts consequently: $\mu(A_{12}) \geq \mu(A_{13})$.

Now what remains is to address the case for $\alpha > 1$. In this case we will have that $p_1^{\alpha-1} - p_2^{\alpha-1} > 0$, so that the derivative of S with respect to d will be:

$$\frac{dS}{d|\rho|} = \text{Positive constant} \times (\text{Positive quantity}) = \text{Positive}.$$

Thus, $\frac{dS}{d|\rho|} > 0$ when $\alpha > 1$. Taking the derivative of $H_\alpha(P)$ with Respect to $|\rho|$:

$$\frac{dH}{d|\rho|} = \frac{1}{1-\alpha} \cdot \frac{1}{S} \cdot \frac{dS}{d|\rho|}.$$

Since $\frac{dS}{d|\rho|} > 0$ and $S > 0$, the sign of $\frac{dH}{d|\rho|}$ depends on $\frac{1}{1-\alpha}$, and for $\alpha > 1$, obviously $1 - \alpha < 0 \implies \frac{1}{1-\alpha} < 0$. Therefore, $\frac{dH}{d|\rho|} < 0$. $H_\alpha(P)$ decreases as $|\rho|$ increases even when $\alpha > 1$, regardless of the variances of the variables. Therefore, if $|\rho_{12}| \geq |\rho_{13}|$, then our entropy-based measure of connectedness acts consequently: $\mu(A_{12}) \geq \mu(A_{13})$.

□

4 Connection between Rényi entropy measures and the other proper measures of connectedness

The Market Rank Indicator introduced in Figini et al. (2018) was conceptualized as a generalization of the condition number of a matrix. It considers the k smallest singular values through a geometric mean, rather than just the smallest singular value. This approach shifts the focus to the smaller eigenvalues of the covariance matrix, unlike previous methods such as Billio et al. (2012), which emphasized the larger eigenvalues.

The underlying intuition was that, before and during systemic stock market crashes, an increasing number of stocks become correlated to the point of near-linear dependence (excluding noise), leading to a growing loss of diversification opportunities.

This intuition also inspired indicators based on Chisini means, introduced in Maggi et al. (2020), which generalize the Market Rank Indicator. These indicators have two main weaknesses. First, the parameter governing the number of at-risk diversification opportunities—the number of singular values involved in the indicator—is not endogenous. Second, these indicators decrease as the number of considered singular values increases, which is counterintuitive to the fundamental idea behind the indicators.

To address these weaknesses, Qyrana et al. (2024) propose an indicator that directly counts the number of at-risk diversification opportunities using a threshold to identify the number of near-zero eigenvalues in the correlation matrix. The drawback of this indicator is its discrete nature, which, for a low number of components in the initial matrix, fails to provide sufficiently smooth value transitions.

The EC indicator introduced in this work aims to reconcile the consideration of both the larger and smaller eigenvalues of covariance matrices. It also addresses the challenge of counting the number of eigenvalues dangerously close to zero, and by extension, the number of at-risk diversification opportunities.

To understand how EC naturally continues the concepts developed therein, it is first necessary to present two simple related results.

In particular, we will first show that EC is minimized when the eigenvalues are equal to each other. Due to the inverse monotonicity between EC and the Rényi entropy measure, this is equivalent to showing that entropy is maximized when the probability distribution derived from the eigenvalues, as defined by EC, is uniform.

Secondly, we will demonstrate that, conversely, EC is maximized when the trace of the covariance matrix tends to concentrate on a single eigenvalue, with the others approaching zero. By similar reasoning, this is equivalent to showing that entropy is minimized when the probability distribution derived from the eigenvalues, as defined by EC, tends towards a Kronecker delta.

Let $P = \{p_1, p_2, \dots, p_n\}$ be a discrete probability distribution over a finite set of size n , where $p_i > 0$ and $\sum_{i=1}^n p_i = 1$, then we will focus again on the Rényi entropy of order α (with $\alpha > 0$ and $\alpha \neq 1$) part of our entropy-based connectedness indicator:

$$H_\alpha(P) = \frac{1}{1-\alpha} \log \left(\sum_{i=1}^n p_i^\alpha \right) \quad (5)$$

Proposition 4.1. *The EC is minimized if the probabilities $p_i = \frac{1}{n}$ for all i , i.e. if the distribution probability is uniform.*

Proof. First we want to show that $H_\alpha(P) \leq \log n$, and that equality is reached if and only if $p_i = \frac{1}{n}$ for all i . Again we have to distinguish two cases based on α value. We start from $0 \leq \alpha < 1$. In this range, the function $f(p) = p^\alpha$ is *concave* on $[0, \infty)$ because its second derivative is negative:

$$\frac{d^2}{dp^2} f(p) = \alpha(\alpha - 1)p^{\alpha-2} < 0$$

By Jensen's inequality for concave functions:

$$\sum_{i=1}^n \frac{1}{n} f(p_i) \leq f \left(\sum_{i=1}^n \frac{1}{n} p_i \right)$$

Since $\sum_{i=1}^n \frac{1}{n} p_i = \frac{1}{n} \cdot 1 = \frac{1}{n}$, we have:

$$\frac{1}{n} \sum_{i=1}^n p_i^\alpha \leq \left(\frac{1}{n} \right)^\alpha$$

Multiplying both sides by n :

$$\sum_{i=1}^n p_i^\alpha \leq n^{1-\alpha}$$

Taking the logarithm:

$$\log \left(\sum_{i=1}^n p_i^\alpha \right) \leq (1-\alpha) \log n$$

Therefore:

$$H_\alpha(P) = \frac{1}{1-\alpha} \log \left(\sum_{i=1}^n p_i^\alpha \right) \leq \log n$$

By Jensen's inequality we know that equality holds if and only if $p_i = \frac{1}{n}$ for all i . This can be easily verified:

$$\log \left(\sum_{i=1}^n p_i^\alpha \right) = \log \left(n \left(\frac{1}{n} \right)^\alpha \right) = \log(n) + \log \left(\frac{1}{n} \right)^\alpha = \log(n) + \alpha(\log 1 - \log n) = (1-\alpha)\log(n)$$

Now we deal with the second case given by $\alpha > 1$. Here, $f(p) = p^\alpha$ is *convex* because:

$$\frac{d^2}{dp^2} f(p) = \alpha(\alpha-1)p^{\alpha-2} > 0$$

Then for convex functions Jensen's inequality switch its sign:

$$\sum_{i=1}^n \frac{1}{n} f(p_i) \geq f \left(\sum_{i=1}^n \frac{1}{n} p_i \right)$$

This implies:

$$\frac{1}{n} \sum_{i=1}^n p_i^\alpha \geq \left(\frac{1}{n} \right)^\alpha$$

Multiplying both sides by n :

$$\sum_{i=1}^n p_i^\alpha \geq n^{1-\alpha}$$

Taking the logarithm:

$$\log \left(\sum_{i=1}^n p_i^\alpha \right) \geq (1-\alpha)\log n$$

Since $1-\alpha < 0$, multiplying both sides by $\frac{1}{1-\alpha} < 0$ reverses the inequality:

$$H_\alpha(P) = \frac{1}{1-\alpha} \log \left(\sum_{i=1}^n p_i^\alpha \right) \leq \log n$$

Again, equality holds if and only if $p_i = \frac{1}{n}$ for all i . \square

Proposition 4.2.

$$\sup \mu(A) = \sup \left(\frac{1}{1+H_\alpha(P)} \right) = \lim_{p_j \rightarrow 1_{j \in \{1, \dots, n\}}} \frac{1}{1 + \frac{1}{1-\alpha} \log (\sum_{i=1}^n p_i^\alpha)} \quad (6)$$

Proof. We will focus on $\log (\sum_{i=1}^n p_i^\alpha)$. Being $p_i > 0$ and $\sum_{i=1}^n p_i = 1$, then we can show that the infimum of the Rényi entropy $H_\alpha(P)$ is zero, approached as one of the probabilities tends to 1, and the others tend to 0 while remaining positive.

To do this, without loss of generality, we rewrite the probabilities p_i as:

$$p_1 = \lim_{\epsilon \rightarrow 0} 1 - \epsilon, \quad p_i = \lim_{\epsilon \rightarrow 0} \frac{\epsilon}{n-1} \quad \text{for } i = 2, \dots, n,$$

In this way we obtain for the sum under the logarithm:

$$\sum_{i=1}^n p_i^\alpha = \lim_{\epsilon \rightarrow 0} (1 - \epsilon)^\alpha + (n - 1) \left(\lim_{\epsilon \rightarrow 0} \frac{\epsilon}{n - 1} \right)^\alpha.$$

Now it is convenient to simplify the second term as follows:

$$(n - 1) \left(\frac{\epsilon}{n - 1} \right)^\alpha = (n - 1) \left(\frac{\epsilon^\alpha}{(n - 1)^\alpha} \right) = \frac{\epsilon^\alpha}{(n - 1)^{\alpha-1}}.$$

Now we focus on the first term, expanding it in Taylor's series:

$$(1 - \epsilon)^\alpha = 1 - \alpha\epsilon + \frac{\alpha(\alpha - 1)}{2}\epsilon^2 - \frac{\alpha(\alpha - 1)(\alpha - 2)}{6}\epsilon^3 + \dots$$

In this way we have that:

$$\lim_{\epsilon \rightarrow 0} (1 - \epsilon)^\alpha = 1 - \alpha\epsilon$$

In the limit $\epsilon \rightarrow 0$, the term $\frac{\epsilon^\alpha}{(n - 1)^{\alpha-1}}$ is negligible with respect to $(1 - \epsilon)^\alpha$, so that we are left only with:

$$\sum_{i=1}^n p_i^\alpha \approx 1 - \alpha\epsilon.$$

Now we substitute what we got into the Rényi entropy formula:

$$H_\alpha(P) \approx \frac{1}{1 - \alpha} \log(1 - \alpha\epsilon).$$

Then, expanding in Taylor series $\log(1 - \alpha\epsilon)$ around $\epsilon = 0$ and taking the limit for $\epsilon \rightarrow 0$, we get:

$$\log(1 - \alpha\epsilon) \approx -\alpha\epsilon.$$

So that:

$$\lim_{\epsilon \rightarrow 0} H_\alpha(P) \approx \lim_{\epsilon \rightarrow 0} \frac{\alpha\epsilon}{\alpha - 1} = 0.$$

□

When all eigenvalues tend to be equivalent, it means that there are no components in the reference market that are more or less important than others, and thus all are necessary to contribute to market diversification. In the extreme opposite case, it would mean that there is a market component whose behavior is strongly mimicked by all others, making them redundant.

Considering the MRI and other measures based on Chisini means, for a fixed number of singular values to be considered for the mean, we observe that the value of these indicators reaches its maximum and minimum under the same conditions as EC.

Regarding the DLI proposed by Qyrana et al. (2024), it similarly reaches its maximum value under the same conditions as EC. However, its behavior is not predefined in the case

of uniform eigenvalues, where it could potentially reach either its maximum or minimum value.

5 Empirical Results

In this section, we detail the experimental setup used in our study. We begin by describing the datasets utilized, followed by a comprehensive explanation of the backtesting methodologies employed. Finally, we present the experiments conducted and discuss the results obtained from these analyses.

5.1 The datasets

For the experiments conducted, we utilize two primary datasets. The first dataset comprises the logarithmic returns of the 10 GICS sectors of the S&P 500 and the logarithmic returns of the S&P 500 index, covering a period of approximately 24 years, from January 4, 1999, to December 29, 2023. The second dataset includes the logarithmic returns of the 10 GICS sectors of the MSCI World and the logarithmic returns of the MSCI World Index, spanning approximately 24 years, from January 2, 2001, to October 14, 2024. Then, we will produce the same analyses on a dataset which is constituted by the logarithmic returns of 10 GICS sectors of the S&P 500 combined with logarithmic returns of the MSCI World Index, then generating a dataset which spans from January 2, 2001 to December 29, 2023. The reasons behind this mixing choice will be clearer in the backtest sections. All observations are on daily basis. Note that we have excluded the Real Estate sector because it was added later compared to the original 10 sectors, which would have necessitated shortening the dataset.

5.2 EC-based investment strategy

First of all, among the general class of EC measures we proposed in this work, we chose for these tests the collision entropy-based proper measure of connectedness, with A being the matrix that collect observations along rows and assets along columns, standardized such to have zero mean and unitary standard deviation. This means that the eigenvalues used to construct the associated probability measures are those of the correlation matrix. Formally the indicator we are using for the empirical experiments is then defined as follows. Let $A \in \mathcal{M}_{T \times n}(\mathbb{R})$ be a full-ranked random matrix where $T > n$ whose column vectors have zero mean and unitary standard deviation, with $\mathcal{M}_{T \times n}(\mathbb{R})$ denoting the set of real matrices of full rank, n representing the number of assets, and T the number of observations. Let $\Xi(A) \in \mathcal{M}_{n \times n}(\mathbb{R})$ denote the empirical covariance matrix of A that is equivalent in this case to the correlation matrix, with eigenvalues $0 \leq \lambda_1 \leq \dots \leq \lambda_n$. Finally let $P = \{p_i\}$ with $p_i = \frac{\lambda_i}{\sum_{j=1}^n \lambda_j}$ and a real parameter $\alpha \geq 0$ (with $\alpha \neq 1$). The indicator we will use in this section will then be:

$$\mu(A) = \frac{1}{1 + H_2(P)} = \frac{1}{1 + \frac{1}{1-2} \log \left(\sum_{i=1}^n p_i^2 \right)} = \frac{1}{1 - \log \left(\sum_{i=1}^n p_i^2 \right)} \quad (7)$$

Our objective is to demonstrate that the proposed index can effectively signal imminent unfavorable investment periods. By enabling an adaptive strategy that reduces portfolio exposure during these periods, this approach aims to outperform a benchmark strategy—defined in our study as investing the entire available capital in the market—over the long term.

To achieve this objective, we formalize our strategy as follows: let $(r_t)_{t=0}^T$ and $(\chi_t)_{t=0}^T$ represent, respectively, the logarithmic return of a portfolio and its profit-loss sequences. Let $(\mu_t)_{t=0}^T \in \mathbb{N}_0$ be the proposed index, which is designed to indicate periods of heightened risk in the market.

We define our investment strategy S by the following rules:

$$\chi_t^S = \begin{cases} m\chi_{t-1}^S e^{r_t} + (1-m)\chi_{t-1}^S, & \text{if } \mu_{t-h} \geq \bar{\mu} \\ \chi_{t-1}^S e^{r_t}, & \text{otherwise} \end{cases} \quad (8)$$

In the formula, h denotes the forecast horizon length, which indicates the number of days between the signal provided by the indicator and the potential deactivation of the investment applied to the portfolio. In our study, we conducted experiments with $h \in \{1, 2\}$.

Then $m \in [0, 1]$ represents the percentage of capital to be invested at time t , and $\bar{\mu}$ is a threshold for the index. The strategy reduces exposure when μ_t exceeds $\bar{\mu}$, indicating a potential unfavorable period.

In simpler terms, this formula suggests that when our index at time $t - h$ μ_{t-h} exceeds the threshold $\bar{\mu}$, only a portion m of the available capital is invested at time t , while the rest is kept as cash.

Our goal is to show that this strategy S leads to better performance compared to a benchmark strategy of full market exposure. Formally, we aim to demonstrate that $\theta(\chi_T^S) > \theta(\chi_T)$, where $\theta : \mathbb{R}^T \rightarrow \mathbb{R}$ is some general performance measure, and T is the final time period.

Following the strategy outlined, two further critical decisions must be addressed: the selection of the warning threshold for the index ($\bar{\mu}$) and the determination of the proportion of capital to be invested at each time t (m).

In the context of this last choice, the investment ratio m is set to 0. This implies that upon surpassing the specified threshold, the entire position in the underlying asset is liquidated, converting all capital into cash. Subsequently, the position is reestablished by reinvesting the total capital once the indicator value reverts to a level below the threshold.

The investment percentage represents a crucial parameter for practitioners aiming to implement the proposed trading strategy. It necessitates thorough analysis to identify optimal levels that balance the exploitation of trading signals with the associated commission

costs. Furthermore, it may be insightful to investigate whether the indicator can function as a variable within a model that maps its values to corresponding investment levels m . Nevertheless, within the scope of this study, the trading strategy serves solely as a framework designed to offer a clear and unbiased assessment of the predictive capabilities of the developed indicator.

In relation to the determination of the threshold μ , we propose an approach analogous to that delineated in Qyrana (2024). The indicator is constructed such that, theoretically, an increase in its value corresponds to an elevated likelihood of a stock market crash. Given that stock market crashes are relatively infrequent events, we combine these insights to derive the threshold as a sufficiently high indicator percentile. In Qyrana (2024), a percentile around the 95th was selected, with iterative adjustments tailored to the indicators under empirical comparison to achieve optimal performances against which to compare the indicator produced in the paper. In this study, we adopt a slightly modified methodology. We evaluate all percentiles from 90.1% to 99%, in increments of 0.1%, and iteratively recalculate performance metrics. This process yields a spectrum of 91 potential equity lines for each indicator, obtained by implementing the previously described strategy based on the indicator's values. This approach aids in assessing the robustness of the proposed indicators with respect to the choice of the disinvestment trigger threshold. Sufficient robustness is desirable because precise knowledge of the indicator's reference percentiles can only be obtained over a sufficiently long period and after observing enough crisis events. Therefore, it is advantageous to have indicators whose behavior does not vary significantly if the threshold is chosen within a reasonable range of values.

5.3 Systemic Risk Indicators for Comparative Analysis

To maintain fairness and avoid contamination in the comparative analysis between the systemic risk indicator proposed in this study and other similar indicators from the literature, based on the previously described trading strategy, we selected indicators that exhibit continuous values and are independent of parameters or hyperparameters lacking an a priori selection criterion. The first characteristic ensures that the comparison, grounded on a sufficiently high number of percentiles, remains meaningful, as discrete-valued indicators would result in buckets of identical strategies. The second characteristic aims to eliminate the introduction of arbitrary degrees of freedom by the author. Consequently, indicators such as ADLI and DLI from Qyrana (2024), MRI from Fignini (2018), and, more broadly, indicators based on Chisini means proposed in Maggi (2020), as well as the Absorption Ratio measure from Billio (2012), were excluded. The indicators selected for this comparative study are Average Correlation and Maximum Eigenvalue, which have been previously employed as benchmark measures in Qyrana (2024).

5.4 Details and notation of backtest analyses

Correlation matrices were estimated using 13-day windows, i.e. $T = 13$, with indicator values linked to returns computed on the closing prices of the 13th and 14th days in the case of $h = 1$, and on the closing prices of the 14th and 15th days in the case of $h = 2$. Then the procedure is iterated in rolling windows with one day step ahead. The number of observations for the correlation matrices estimation was chosen to ensure the windows remain as short as possible, thereby enhancing the indicators' responsiveness and preserving their predictive capabilities.

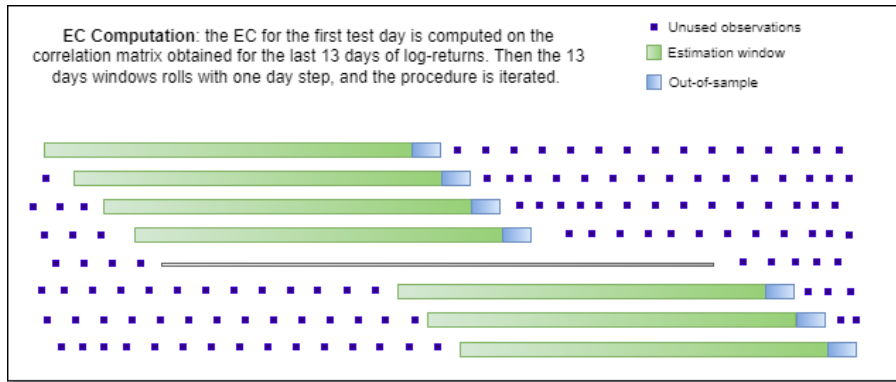


Figure 1: *Walk-forward estimation-backtest scheme, $h = 1$.*

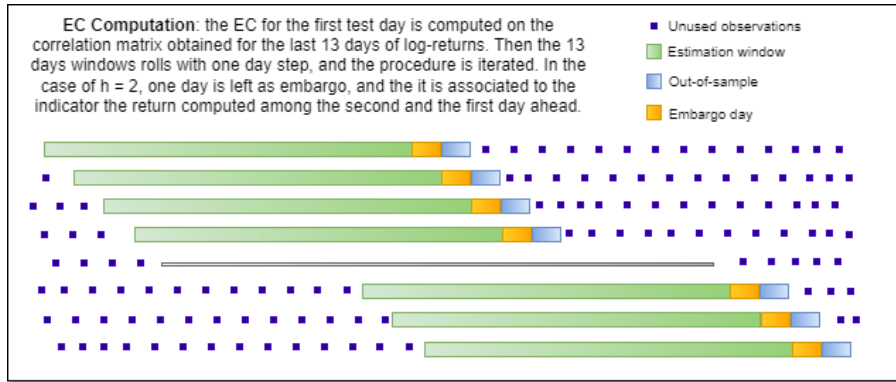


Figure 2: *Walk-forward estimation-backtest scheme, $h = 2$.*

The strategies and performance metrics associated with the EC, Average Correlation, and Maximum Eigenvalue are denoted by the prefixes *EC*, *AC*, and *EV*, respectively, in the charts and tables of the subsequent sections. The results presented in the charts and tables are differentiated by the reference datasets labeled S&P500 and MSCI World Index, which indicate their respective reference universes. We call *Benchmark* the indexes, and *Strategies* or, depending on the context, *Portfolio* (with the due prefix) the indexes on which the filtering strategies based on their underlying systemic risk indicators have been constructed. In the subsequent table, we present a summary of the abbreviations used for various performance, risk, and risk-adjusted performance indicators.

Abbreviation	Metrics
maxD	Maximum Drawdown
meanD	Average Drawdown
VaR	Value at Risk
cVaR	Conditional Value at Risk
mean	Mean Return
std	Standard Deviation
skew	Skewness
kurt	Kurtosis
SR	Sharpe Ratio
ISR	Information Ratio
SoR	Sortino Ratio
CR	Calmar Ratio

In our analysis, we followed an unconventional choice for the drawdown and Value-at-Risk (both unconditional and conditional) measures by retaining the negative sign. As for the mean return, the percentage symbol indicates that the mean logarithmic return has been multiplied by 100. The Value-at-Risk indicators have been computed with a 95% confidence level and with the historical method. Furthermore, we set the risk-free rate equal to zero. The daily mean return has been multiplied by 100. The model with the highest value for each given metric is highlighted in bold. In instances where multiple models yield equivalent values for a specific metric, additional decimal places (not displayed in the tables due to space constraints) were considered to determine the leading model.

5.5 Backtest: case for $h = 1$

In this section, we present experiments conducted with a one-day forecast horizon. This implies that if the indicator exceeds the predetermined threshold at the close of the current day, the capital will not be invested and will remain unaffected by the underlying asset's fluctuations on the following day. This temporal framework allows for the possibility of selling at the close of the current day. This means that 8 becomes:

$$\chi_t^S = \begin{cases} m\chi_{t-1}^S e^{r_t} + (1-m)\chi_{t-1}^S, & \text{if } \mu_{t-1} \geq \bar{\mu} \\ \chi_{t-1}^S e^{r_t}, & \text{otherwise} \end{cases} \quad (9)$$

The remainder of this section is organized according to the datasets on which the backtests are conducted.

5.5.1 S&P500 Sectors and SP500 Index

In this section, the systemic risk indicators are calculated using the 10 GICS sectors of the S&P 500, with the underlying asset for the disinvestment timing strategies being the

S&P 500 index. The chart 3 illustrates how the EC not only helps control risk but also potentially improves returns for the vast majority of adopted thresholds. The tables 1, 2, 3 and 4 respectively indicate the average and median of performance and risk metrics calculated across the bundle of profit and loss curves for each systemic risk indicator.

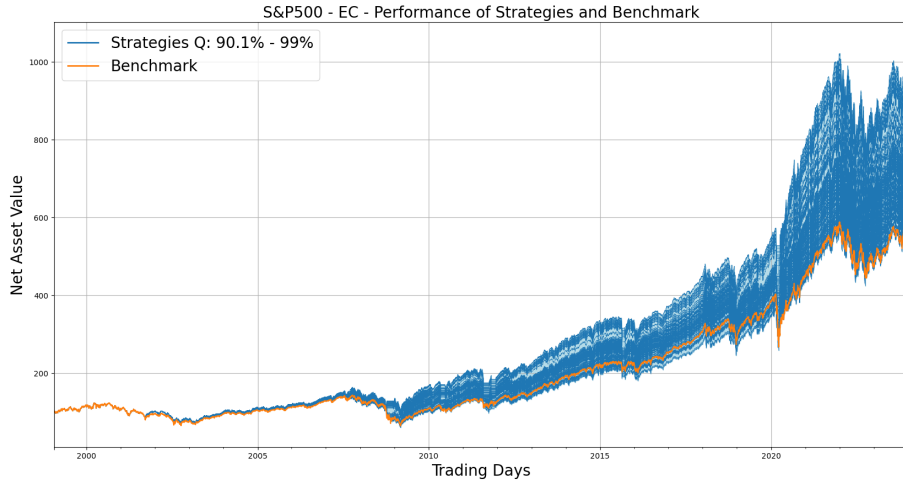


Figure 3: *S&P500, $h = 1$: Profit and Loss curves of strategies based on EC against the Benchmark. The bundle of profit and loss curves of the strategies is obtained by varying the threshold $\bar{\mu}$ along the percentiles from 90% to 99%, in steps of 1%.*

The EC Portfolio demonstrates superior performance on average in terms of mean returns (0.0312) compared to both the AC (0.0304) and EV (0.0306) portfolios, as well as the benchmark (0.0279). This indicates that the EC measure not only helps in risk management but also potentially enhances returns. In terms of risk measures, the EC Portfolio exhibits the lowest maximum drawdown (-0.48) and average drawdown (-0.09), highlighting its effectiveness in controlling downside risk compared to the AC (-0.50 and -0.10) and EV (-0.50 and -0.11) portfolios. The benchmark shows a significantly higher maximum drawdown (-0.55) and average drawdown (-0.11), further emphasizing the risk mitigation capabilities of the EC measure.

Both VaR and cVaR are lower for the EC Portfolio (-0.017 and -0.026) than for the benchmark (-0.019 and -0.030), which suggests better tail risk management by the EC measure. The AC and EV portfolios also show similar VaR and cVaR values, indicating comparable tail risk control among the proposed strategies. The standard deviation of returns (std) for the EC Portfolio (1.055) is slightly lower than that of the AC (1.057) but higher than EV (1.050) portfolios, and significantly lower than the benchmark (1.212).

Table 1: S&P500, $h = 1$: Descriptive Statistics of Portfolios (Part 1)

Average	maxD	meanD	VaR	cVaR	mean	std	skew	kurtosis
EC Portfolio	-0.48	-0.09	-0.017	-0.026	0.0312	1.055	-0.164	6.58
AC Portfolio	-0.50	-0.10	-0.017	-0.026	0.0304	1.057	-0.176	6.48
EV Portfolio	-0.50	-0.11	-0.017	-0.026	0.0306	1.050	-0.20	5.66
Benchmark	-0.55	-0.11	-0.019	-0.030	0.0279	1.212	-0.370	10.50

Table 2: S&P500, $h = 1$: Descriptive Statistics of Portfolios (Part 2)

Average	SR	ISR	SoR	CR
EC Portfolio	0.47	0.09	0.41	0.47
AC Portfolio	0.46	0.07	0.39	0.43
EV Portfolio	0.46	0.08	0.40	0.43
Benchmark	0.37	NaN	0.32	0.36

The median statistics in Table 3 reinforce the observations from the average metrics. The EC Portfolio again shows a higher median mean return (0.0311) compared to the AC (0.0300) and EV (0.0298) portfolios, and the benchmark (0.0279). The EC Portfolio also maintains its advantage in risk measures with a lower median maximum drawdown (-0.44) and average drawdown (-0.09) compared to the AC (-0.47 and -0.10) and EV (-0.48 and -0.10) portfolios. The benchmark remains the worst performer in these metrics.

The EC Portfolio exhibits higher skewness (-0.164) and lower kurtosis (6.58) compared to the benchmark (-0.370 and 10.50), suggesting a distribution of returns that is closer to normal and less prone to extreme and especially negative outcomes. The AC and EV portfolios show similar trends, with the EV Portfolio having the lowest kurtosis.

The EC Portfolio demonstrates the highest Sharpe Ratio (0.47), Information Ratio (0.09), Sortino Ratio (0.41), and Calmar Ratio (0.47) among the strategies and the benchmark. This indicates that the EC measure provides the best risk-adjusted returns. The AC and EV portfolios also show improvements in these metrics compared to the benchmark, but not at the same level of the EC portfolios.

Table 3: S&P500, $h = 1$: Descriptive Statistics of Portfolios (Part 1)

Median	maxD	meanD	VaR	cVaR	mean	std	skew	kurtosis
EC Portfolio	-0.44	-0.09	-0.017	-0.025	0.0311	1.0509	-0.16	6.70
AC Portfolio	-0.47	-0.10	-0.014	-0.022	0.0300	1.05	-0.19	6.67
EV Portfolio	-0.48	-0.10	-0.017	-0.025	0.0298	0.9255	-0.45	5.70
Benchmark	-0.55	-0.11	-0.019	-0.030	0.0279	1.2117	-0.37	10.50

Table 4: S&P500, $h = 1$: Descriptive Statistics of Portfolios (Part 2)

	Median	SR	ISR	SoR	CR
EC Portfolio	0.47	0.09	0.40	0.47	
AC Portfolio	0.46	0.06	0.39	0.44	
EV Portfolio	0.45	0.05	0.39	0.42	
Benchmark	0.37	NaN	0.32	0.36	

To provide a broader perspective on the results, we provide also charts 5 of the distributions of the metrics for the three systemic risk indicators.

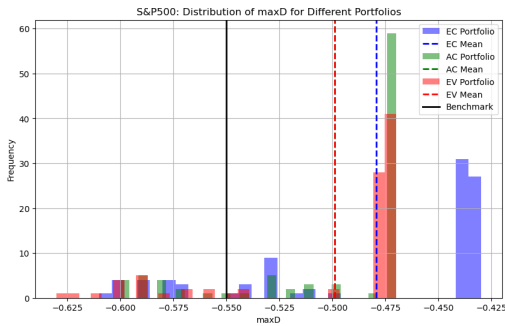


Figure 4: S&P500, $h = 1$: Maximum Drawdown.

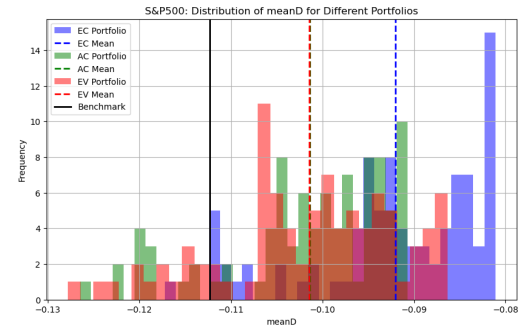


Figure 5: S&P500, $h = 1$: Average Drawdown.

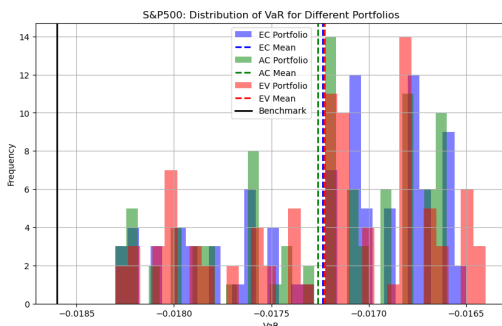


Figure 6: S&P500, $h = 1$: Value-at-Risk.

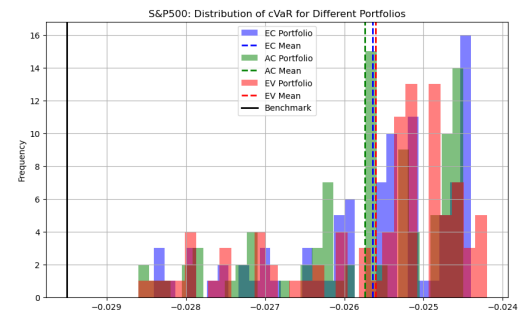


Figure 7: S&P500, $h = 1$: Conditional Value-at-Risk.

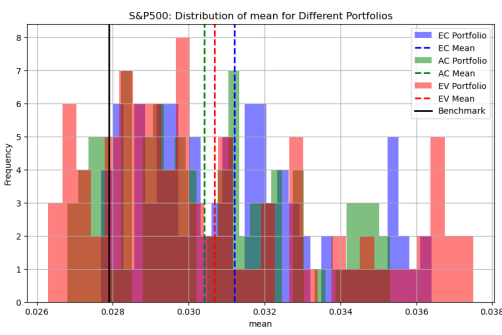


Figure 8: $S\&P500$, $h = 1$: Returns Mean.

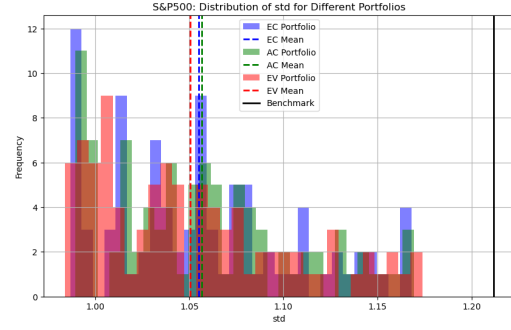


Figure 9: $S\&P500$, $h = 1$: Returns Standard Deviation.

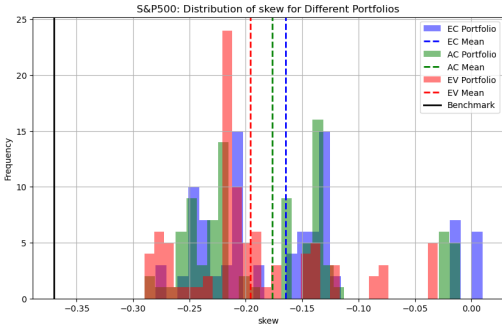


Figure 10: $S\&P500$, $h = 1$: Returns Skewness.

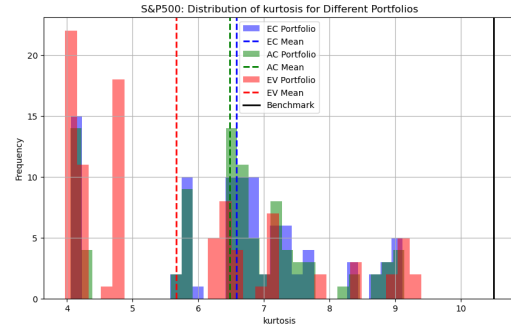


Figure 11: $S\&P500$, $h = 1$: Returns Kurtosis.

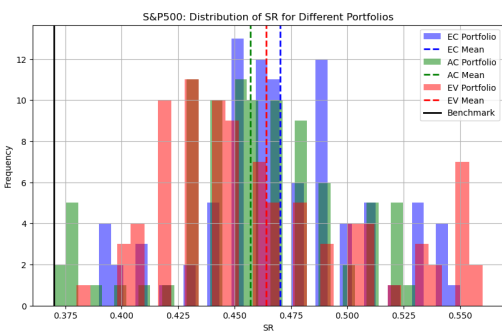


Figure 12: $S\&P500$, $h = 1$: Sharpe Ratio.

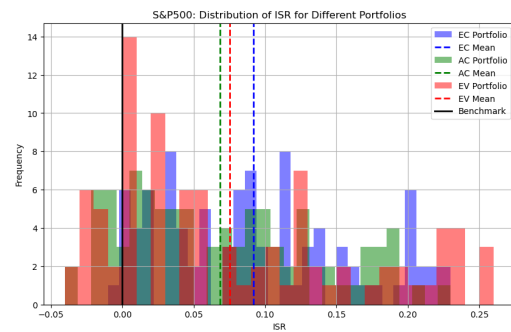


Figure 13: $S\&P500$, $h = 1$: Information Ratio.

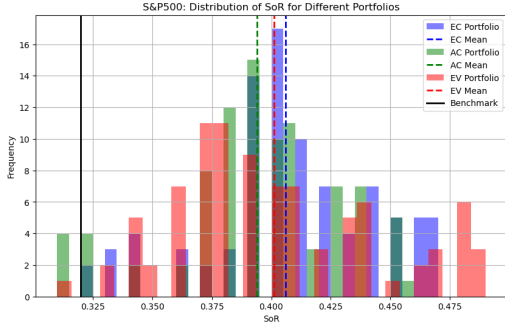


Figure 14: *S&P500, h = 1: Sortino Ratio.*

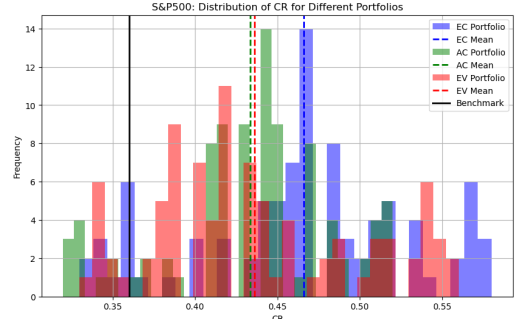


Figure 15: *S&P500, h = 1: Calmar Ratio.*

5.5.2 MSCI World Sectors and MSCI World Index

In this section, the systemic risk indicators are calculated using the 10 GICS sectors of the MSCI World, with the underlying asset for the disinvestment timing strategies being the MSCI World index. The chart 16 shows again the capacity of the EC both to control risk and also to enhance returns for the vast majority of adopted thresholds, even if results appear to be not so good as they was for the S&P500 case. The tables 5, 6, 7 and 8 indicate respectively the average and median performance and risk metrics calculated across the bundle of profit and loss curves for each systemic risk indicator.



Figure 16: *MSCI World, h = 1: Profit and Loss curves of strategies based on EC against the Benchmark. The bundle of profit and loss curves of the strategies is obtained by varying the threshold $\bar{\mu}$ along the percentiles from 90% to 99%, in steps of 1%.*

Table 5: MSCI World, $h = 1$: Descriptive Statistics of Portfolios (Part 1)

Average	maxD	meanD	VaR	cVaR	mean	std	skew	kurtosis
EC Portfolio	-0.56	-0.11	-0.014	-0.022	0.0282	0.915	-0.358	8.84
AC Portfolio	-0.56	-0.11	-0.014	-0.022	0.0281	0.915	-0.356	8.85
EV Portfolio	-0.56	-0.11	-0.014	-0.022	0.0271	0.914	-0.382	8.89
Benchmark	-0.57	-0.11	-0.015	-0.025	0.0270	1.016	-0.600	11.02

 Table 6: MSCI World, $h = 1$: Descriptive Statistics of Portfolios (Part 2)

Average	SR	ISR	SoR	CR
EC Portfolio	0.49	0.04	0.42	0.36
AC Portfolio	0.49	0.04	0.41	0.35
EV Portfolio	0.47	0.01	0.40	0.35
Benchmark	0.42	NaN	0.36	0.33

The EC Portfolio demonstrates slightly higher performance in terms of mean returns (0.0282) compared to the AC (0.0271). In terms of returns, on average the EV portfolios (0.0273) were less performative, as well as the benchmark (0.0270). In terms of risk measures, the EC Portfolio exhibits a maximum drawdown (-0.56) and average drawdown (-0.11) that are comparable to those of the AC (-0.56 and -0.11) and EV (-0.58 and -0.11) portfolios, and slightly better than the benchmark (-0.57 and -0.11).

Both VaR and cVaR are lower for the EC Portfolio (-0.014 and -0.022) than for the benchmark (-0.015 and -0.025), suggesting better tail risk management by the EC measure. The AC and EV portfolios also show similar VaR and cVaR values (-0.014 and -0.022), indicating comparable tail risk control among the proposed strategies. The standard deviation of returns (std) for the EC Portfolio (0.915) is slightly lower than that of the AC (0.915) but higher than EV (0.914) portfolios, and significantly lower than the benchmark (1.016). In terms of ratios, the EC Portfolio wins by a narrow margin with respect to all four metrics.

 Table 7: MSCI World, $h = 1$: Descriptive Statistics of Portfolios (Part 1)

Median	maxD	meanD	VaR	cVaR	mean	std	skew	kurtosis
EC Portfolio	-0.56	-0.10	-0.014	-0.022	0.0283	0.9029	-0.31	7.47
AC Portfolio	-0.56	-0.10	-0.014	-0.022	0.0283	0.9031	-0.31	7.44
EV Portfolio	-0.56	-0.10	-0.014	-0.023	0.0275	0.9033	-0.42	9.43
Benchmark	-0.57	-0.11	-0.015	-0.025	0.0270	1.0159	-0.60	11.02

Table 8: MSCI World, $h = 1$: Descriptive Statistics of Portfolios (Part 2)

	Median	SR	ISR	SoR	CR
EC Portfolio	0.49	0.04	0.41	0.35	
AC Portfolio	0.49	0.05	0.41	0.35	
EV Portfolio	0.48	0.01	0.41	0.36	
Benchmark	0.42	NaN	0.36	0.33	

The median statistics reinforce the observations from the mean metrics, while showing an improvement for the metrics of the EV Portfolios. The EC Portfolio shows a median return (0.0283) that is comparable to the AC (0.0283) and EV (0.0275) portfolios, and higher than the benchmark (0.0270). The EC Portfolio also maintains its advantage in risk measures with a lower median maximum drawdown (-0.56) and average drawdown (-0.10) compared to the AC and EV portfolios. The benchmark remains the worst performer in these metrics.

The EC Portfolio exhibits on average skewness (-0.358) and kurtosis (8.84) that are respectively lower than the benchmark (-0.600 and 11.02), suggesting a distribution of returns that is closer to normal and less prone to extreme outcomes, especially negative ones. The AC portfolios show similar trends, while the EV ones have higher kurtosis (10.08), indicating a higher propensity for extreme returns.

As for the risk-adjusted performances ratios, the EC Portfolios do slightly better in terms of Sharpe and Sortino Ratio, while for the Information Ratio the AC Portfolio obtains the best result and the EV Portfolio wins for the Calmar Ratio.

Figure 18 depicts the distributions of the metrics for the three systemic risk indicators portfolios.

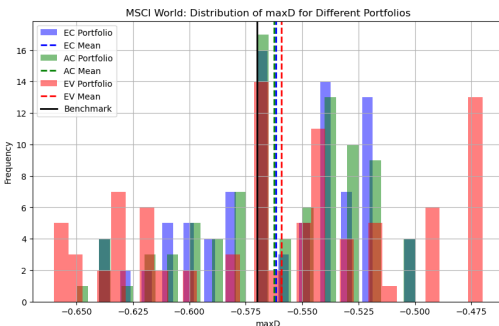


Figure 17: *MSCI World, $h = 1$: Maximum Drawdown.*

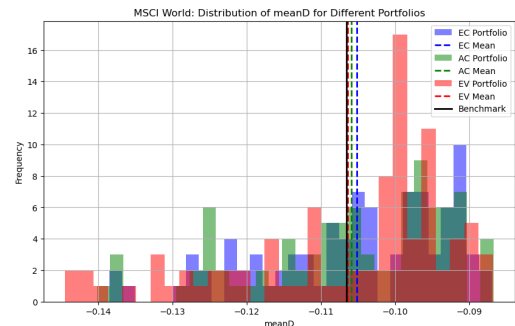


Figure 18: *MSCI World, $h = 1$: Average Drawdown.*

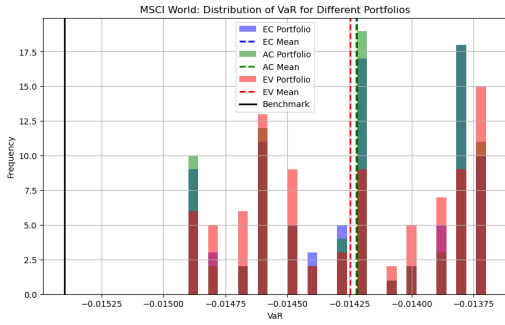


Figure 19: *MSCI World, h = 1: Value-at-Risk.*

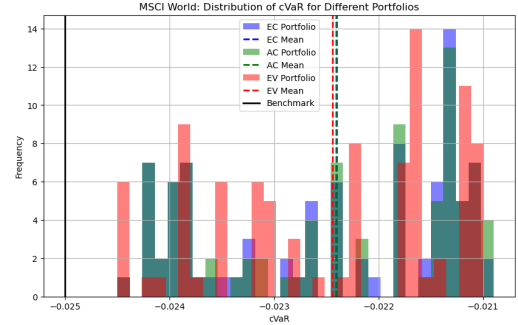


Figure 20: *MSCI World, h = 1: Conditional Value-at-Risk.*

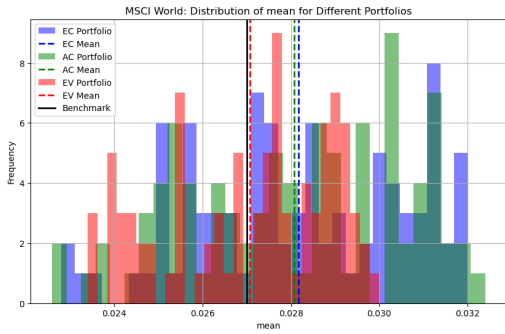


Figure 21: *MSCI World, h = 1: Returns Mean.*

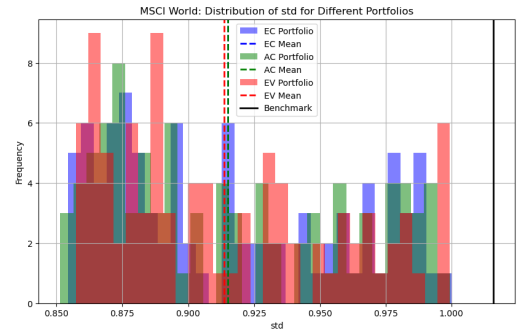


Figure 22: *MSCI World, h = 1: Returns Standard Deviation.*

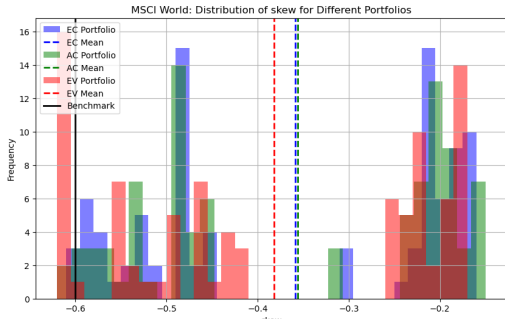


Figure 23: *MSCI World, h = 1: Returns Skewness.*

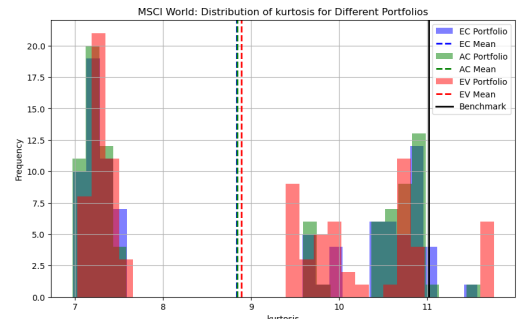


Figure 24: *MSCI World, h = 1: Returns Kurtosis.*

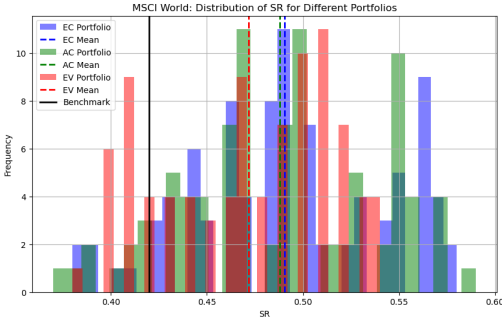


Figure 25: *MSCI World, h = 1: Sharpe Ratio.*

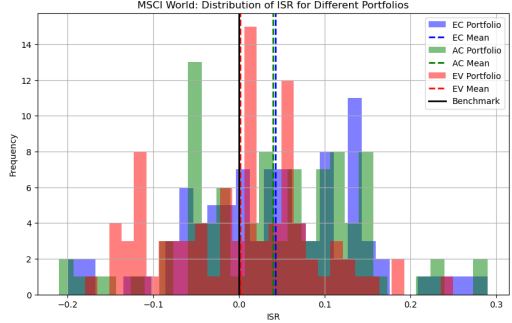


Figure 26: *MSCI World, h = 1: Information Ratio.*

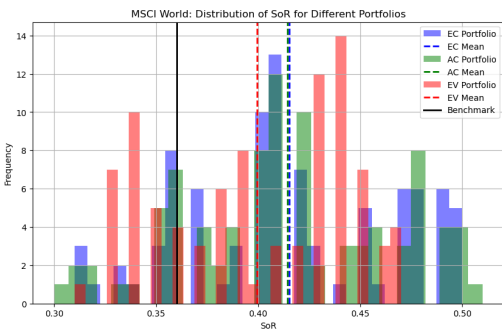


Figure 27: *MSCI World, h = 1: Sortino Ratio.*

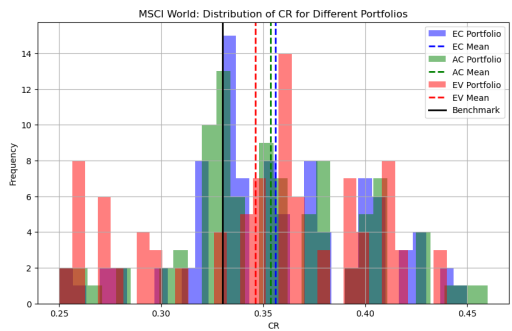


Figure 28: *MSCI World, h = 1: Calmar Ratio.*

5.5.3 S&P500 Sectors and MSCI World Index

It is evident that the indicators have performed better for the S&P500 index compared to the MSCI World index. Given that the S&P500 constituents account for over 50% of the MSCI World index in terms of weight, this marked difference in behavior warrants further investigation. Therefore, in this section, we propose an experiment by cross-referencing the datasets: we will compute the correlation matrices on the logarithmic returns of the 10 GICS sectors of the S&P500, while applying the indicator-based strategies to the MSCI World index. The chart ?? makes it evident how using the EC on the S&P500 sectors yields far better results for the prediction of MSCI World index crashes. The tables 9, 10, 11 and 12 show that this result holds also for the AC and EV portfolios.

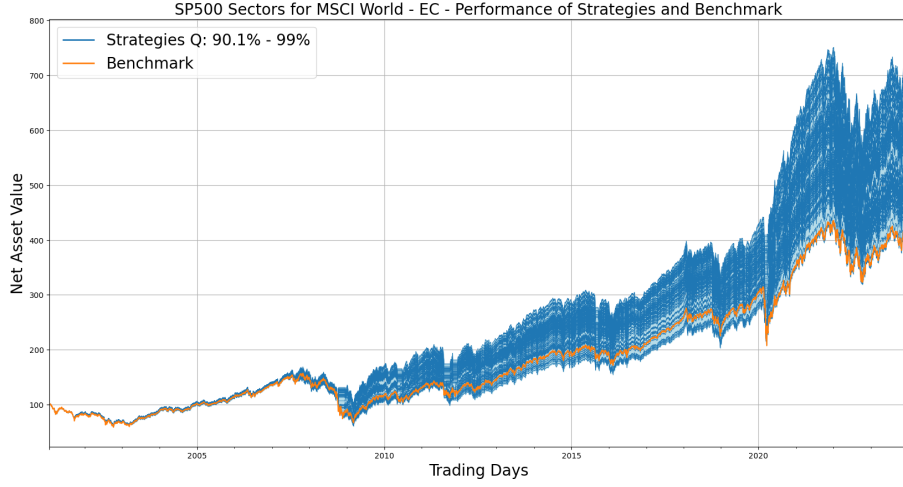


Figure 29: *S&P500 sectors MSCI World, $h = 1$: Profit and Loss curves of strategies based on EC against the Benchmark. The bundle of profit and loss curves of the strategies is obtained by varying the threshold $\bar{\mu}$ along the percentiles from 90% to 99%, in steps of 1%.*

Table 9: S&P500 sectors MSCI World, $h = 1$: Descriptive Statistics of Portfolios (Part 1)

Average	maxD	meanD	VaR	cVaR	mean	std	skew	kurtosis
EC Portfolio	-0.48	-0.087	-0.014	-0.022	0.0299	0.890	-0.214	7.15
AC Portfolio	-0.49	-0.091	-0.014	-0.022	0.0294	0.891	-0.213	7.01
EV Portfolio	-0.48	-0.092	-0.014	-0.022	0.0289	0.885	-0.280	6.13
Benchmark	-0.57	-0.110	-0.016	-0.025	0.0249	1.025	-0.590	10.94

Table 10: S&P500 sectors MSCI World, $h = 1$: Descriptive Statistics of Portfolios (Part 2)

Average	SR	ISR	SoR	CR
EC Portfolio	0.54	0.15	0.47	0.45
AC Portfolio	0.53	0.14	0.46	0.44
EV Portfolio	0.52	0.12	0.45	0.43
Benchmark	0.39	NaN	0.33	0.31

The analysis reveals that all three indicator-based portfolios (EC, AC, and EV) outperform the benchmark in terms of risk-adjusted returns. Specifically, the EC Portfolio clearly exhibits the highest mean return (0.0299 average, 0.0303 median) among the portfolios. Additionally, the EC Portfolio shows a significantly lower maximum drawdown (-0.481 average, -0.44 median) compared to the benchmark (-0.570) as well to the AC and EV

ones, indicating superior risk management.

In terms of volatility, the EC Portfolio presents a lower standard deviation (0.890 average, 0.880 median) compared to the benchmark (1.025). The other portfolios, AC and EV, also show reduced volatility relative to the benchmark, with the EV one in particular showing the lowest value. The average drawdown (meanD) and Value at Risk (VaR) metrics further corroborate the enhanced risk control offered by the EC and AC indicators, with values consistently lower than those of the benchmark.

The skewness and kurtosis metrics indicate a more symmetric return distribution for the EC and AC portfolios, compared to the benchmark which shows a higher negative skewness (-0.590) and elevated kurtosis (10.94). This suggests that the benchmark is more prone to extreme negative returns. In contrast, the EC and AC portfolios exhibit lower skewness and kurtosis, indicating more stable and predictable performance.

Table 11: S&P500 sectors MSCI World, $h = 1$: Descriptive Statistics of Portfolios (Part 1)

Median	maxD	meanD	VaR	cVaR	mean	std	skew	kurtosis
EC Portfolio	-0.44	-0.081	-0.014	-0.021	0.0303	0.880	-0.16	6.81
AC Portfolio	-0.44	-0.088	-0.014	-0.021	0.0289	0.883	-0.17	6.76
EV Portfolio	-0.45	-0.089	-0.014	-0.022	0.0276	0.873	-0.27	5.11
Benchmark	-0.57	-0.110	-0.016	-0.025	0.0249	1.025	-0.59	10.94

Table 12: S&P500 sectors MSCI World, $h = 1$: Descriptive Statistics of Portfolios (Part 2)

	Median	SR	ISR	SoR	CR
EC Portfolio	0.54	0.15	0.48	0.46	
AC Portfolio	0.53	0.13	0.47	0.45	
EV Portfolio	0.51	0.10	0.46	0.45	
Benchmark	0.39	NaN	0.33	0.31	

As for the risk-adjusted performance the EC Portfolio achieves the highest ratios with respect to all the other competitor portfolios

Overall, the empirical results demonstrate that the EC indicator provides the most favorable risk-return profile, with lower drawdowns, higher returns, and better risk-adjusted performance metrics across both average and median values. The AC indicator also performs well but clearly underperforms compared to the EC indicator. The EV indicator, while outperforming the benchmark, does not achieve the same level of performance as the EC and AC indicators.

The following graphs provide broader information about the metrics distributions across the possible thresholds.

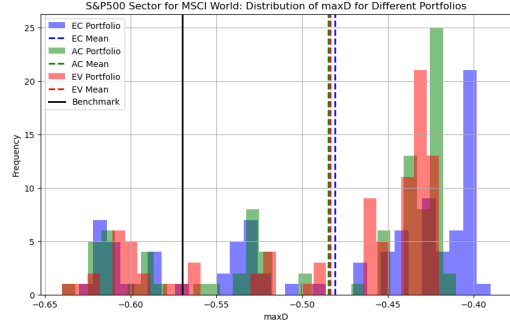


Figure 30: *S&P500 sectors × MSCI World, $h = 1$: Maximum Drawdown Distribution.*

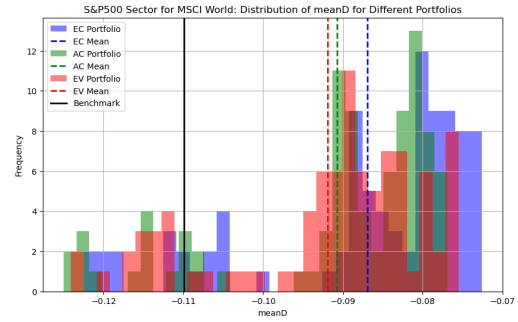


Figure 31: *S&P500 sectors × MSCI World, $h = 1$: Average Drawdown Distribution.*

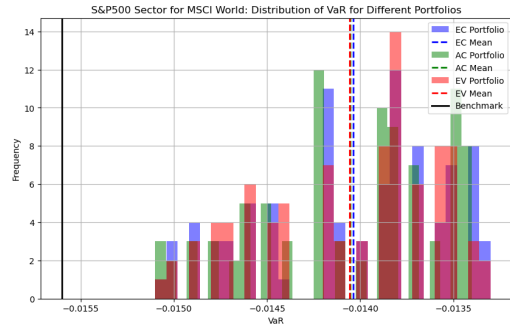


Figure 32: *S&P500 sectors × MSCI World, $h = 1$: Value-at-Risk.*

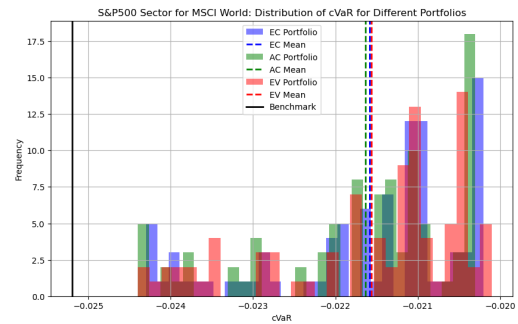


Figure 33: *S&P500 sectors × MSCI World, $h = 1$: Conditional Value-at-Risk.*

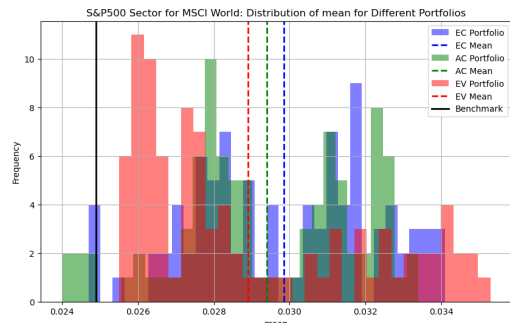


Figure 34: *S&P500 sectors × MSCI World, $h = 1$: Returns Mean.*

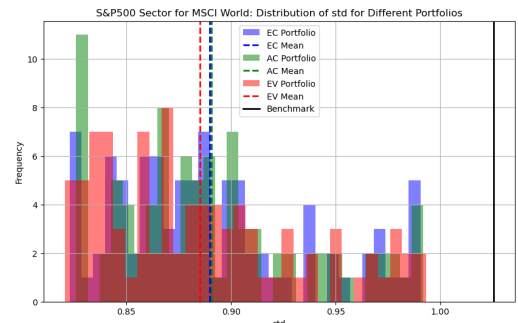


Figure 35: *S&P500 sectors × MSCI World, $h = 1$: Returns Standard Deviation.*

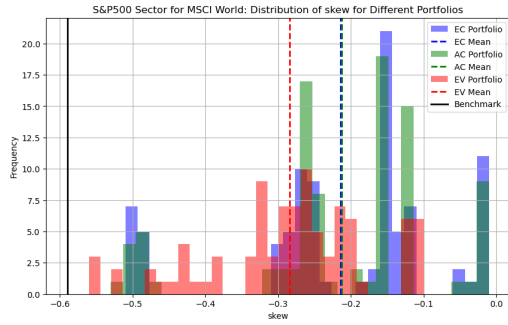


Figure 36: $S\&P500$ sectors \times $MSCI$ World,
 $h = 1$: Returns Skewness.

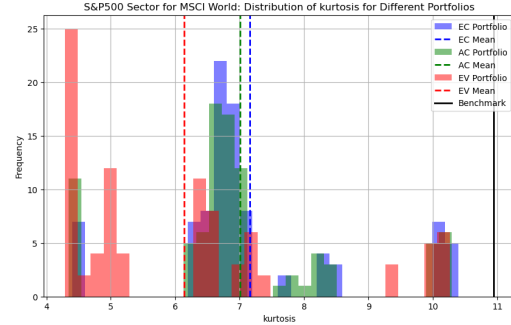


Figure 37: $S\&P500$ sectors \times $MSCI$ World,
 $h = 1$: Returns Kurtosis.

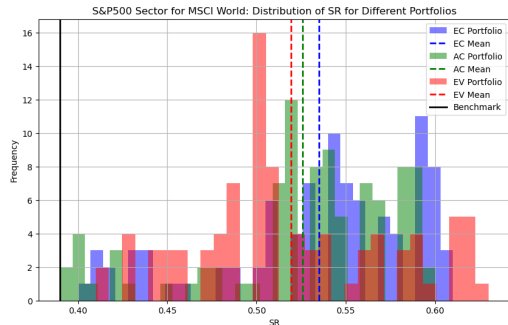


Figure 38: $S\&P500$ sectors \times $MSCI$ World,
 $h = 1$: Sharpe Ratio.

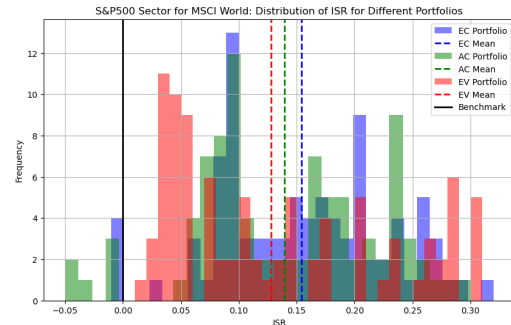


Figure 39: $S\&P500$ sectors \times $MSCI$ World,
 $h = 1$: Information Ratio.

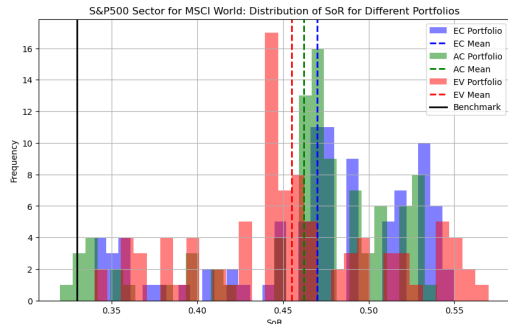


Figure 40: $S\&P500$ sectors \times $MSCI$ World,
 $h = 1$: Sortino Ratio.

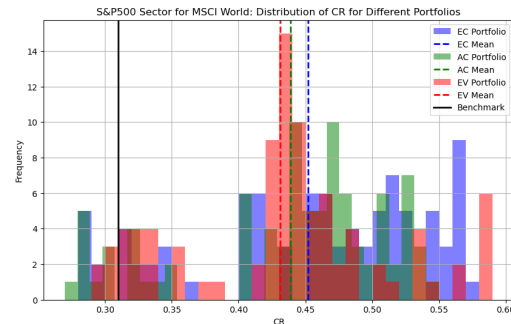


Figure 41: $S\&P500$ sectors \times $MSCI$ World,
 $h = 1$: Calmar Ratio.

5.6 Backtest: case for $h = 2$

In this section, we present experiments conducted with a two-days forecast horizon. This implies that if the indicator exceeds the predetermined threshold at the close of the current day, the position will be closed at the close price of the next day, and the capital will remain unaffected by the underlying asset's fluctuations at least for the time going from the next

day close until the second day ahead close. This means that 8 becomes:

$$\chi_t^S = \begin{cases} m\chi_{t-1}^S e^{r_t} + (1-m)\chi_{t-1}^S, & \text{if } \mu_{t-2} \geq \bar{\mu} \\ \chi_{t-1}^S e^{r_t}, & \text{otherwise} \end{cases} \quad (10)$$

Similarly for the case of $h = 1$, the remainder of this section is organized according to the datasets on which the backtests are conducted.

5.6.1 S&P500 Sectors and SP500 Index

As for the corresponding section for the case of $h = 1$, we calculate the indicators on the 10 GICS sectors of the S&P 500, testing their performance on the S&P 500 index. The chart 42 illustrates how the EC not only helps control risk but also potentially improves returns for the vast majority of adopted thresholds. The tables 13, 14, 15 and 16 respectively indicate the average and median of performance and risk metrics calculated across the bundle of profit and loss curves for each systemic risk indicator.

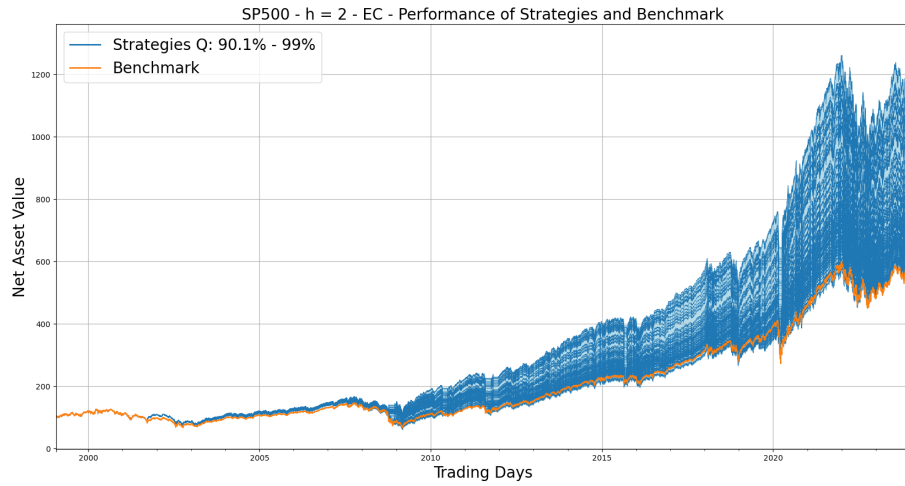


Figure 42: *S&P500, $h = 2$: Profit and Loss curves of strategies based on EC against the Benchmark. The bundle of profit and loss curves of the strategies is obtained by varying the threshold $\bar{\mu}$ along the percentiles from 90% to 99%, in steps of 1%.*

The analysis reveals that the EC Portfolio consistently outperforms the AC and EV portfolios, as well as the benchmark, in terms of pure returns, risk-adjusted returns and drawdown metrics. Specifically, the EC Portfolio exhibits the highest mean return (0.0324 average, 0.0313 median) among the portfolios, showing at the same time a significantly lower maximum and average drawdown compared to both the AC and EV portfolios, and the benchmark (-0.550).

The standard deviation of the EC Portfolio is slightly lower than that of the AC and EV: This dominance with respect to both returns mean and standard deviation is reflected by the fact that the EC portfolio dominates in terms of all risk-adjusted performance indicators.

As for the Value at Risk and Conditional Value at Risk, both metrics are comparable across the EC, AC, and EV portfolios but remain consistently better than those of the benchmark, indicating better downside protection.

Table 13: S&P500, $h = 2$: Descriptive Statistics of Portfolios (Part 1)

Average	maxD	meanD	VaR	cVaR	mean	std	skew	kurtosis
EC Portfolio	-0.46	-0.085	-0.017	-0.026	0.0324	1.049	-0.179	5.69
AC Portfolio	-0.50	-0.106	-0.017	-0.026	0.0301	1.050	-0.203	5.65
EV Portfolio	-0.50	-0.106	-0.017	-0.026	0.0298	1.050	-0.301	6.72
Benchmark	-0.55	-0.112	-0.019	-0.030	0.0281	1.212	-0.370	10.50

Table 14: S&P500, $h = 2$: Descriptive Statistics of Portfolios (Part 2)

Average	SR	ISR	SoR	CR
EC Portfolio	0.49	0.12	0.42	0.50
AC Portfolio	0.47	0.08	0.40	0.43
EV Portfolio	0.45	0.06	0.37	0.42
Benchmark	0.37	NaN	0.32	0.36

The skewness and kurtosis metrics suggest a clearly more favorable return distribution for the EC Portfolio. The EC Portfolio exhibits lower skewness (-0.179 average, -0.19 median) and kurtosis (5.69 average, 4.78 median) compared to the benchmark, and the results are also better than those of the concurrent portfolios, with the exception of the lower kurtosis of the EV portfolio.

Table 15: S&P500, $h = 2$: Descriptive Statistics of Portfolios (Part 1)

Median	maxD	meanD	VaR	cVaR	mean	std	skew	kurtosis
EC Portfolio	-0.42	-0.084	-0.017	-0.025	0.0313	1.037	-0.19	4.78
AC Portfolio	-0.48	-0.104	-0.017	-0.025	0.0298	1.040	-0.21	4.80
EV Portfolio	-0.48	-0.100	-0.017	-0.026	0.0290	1.060	-0.27	6.99
Benchmark	-0.55	-0.112	-0.019	-0.030	0.0281	1.212	-0.37	10.50

Table 16: S&P500, $h = 2$: Descriptive Statistics of Portfolios (Part 2)

	Median	SR	ISR	SoR	CR
EC Portfolio	0.48	0.10	0.42	0.50	
AC Portfolio	0.45	0.04	0.40	0.43	
EV Portfolio	0.44	0.06	0.38	0.41	
Benchmark	0.37	NaN	0.32	0.36	

To provide a broader perspective on the results, we provide also charts 43 of the distributions of the metrics for the three systemic risk indicators.

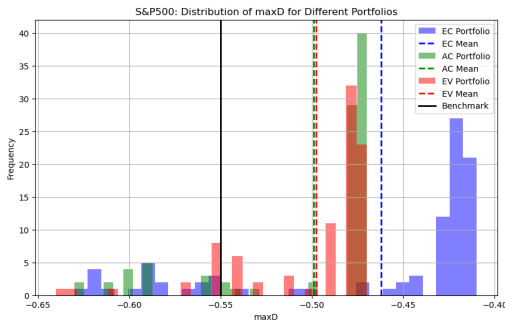


Figure 43: *S&P500, $h = 2$: Maximum Drawdown Distribution.*

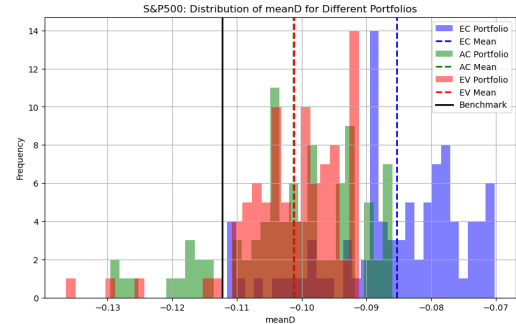


Figure 44: *S&P500, $h = 2$: Average Drawdown Distribution.*

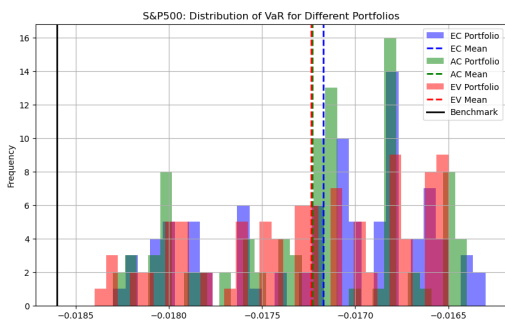


Figure 45: *S&P500, $h = 2$: Value-at-Risk.*

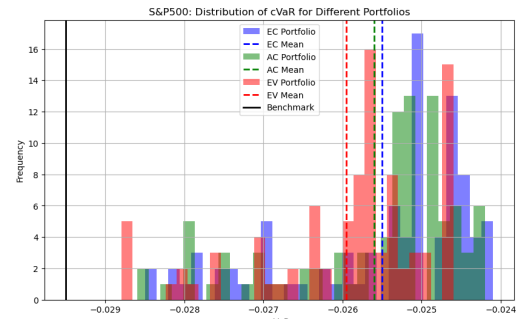


Figure 46: *S&P500, $h = 2$: Conditional Value-at-Risk.*

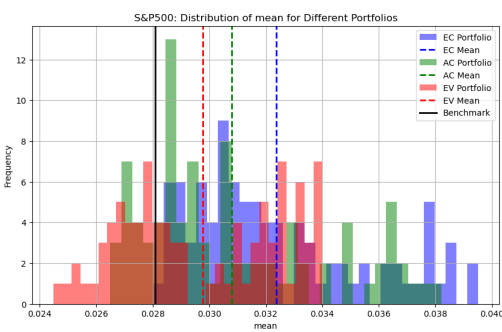


Figure 47: $S\mathcal{E}P500$, $h = 2$: Returns Mean.

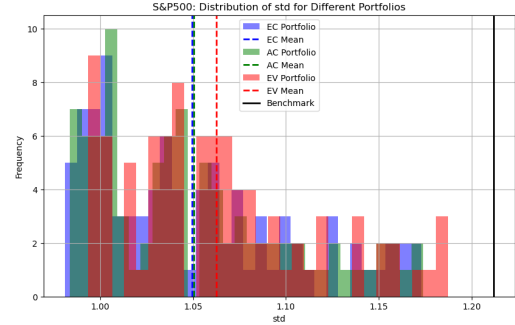


Figure 48: $S\mathcal{E}P500$, $h = 2$: Returns Standard Deviation.

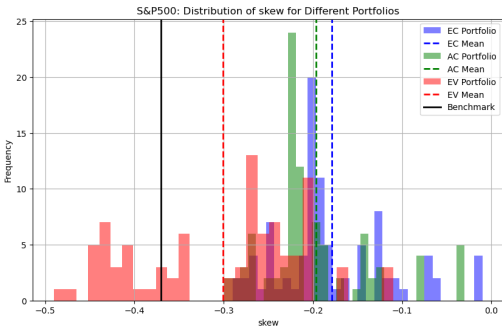


Figure 49: $S\mathcal{E}P500$, $h = 2$: Returns Skewness.

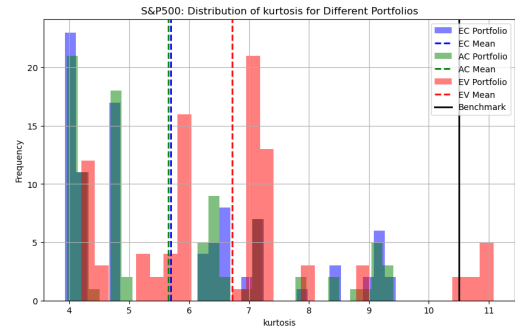


Figure 50: $S\mathcal{E}P500$, $h = 2$: Returns Kurtosis.

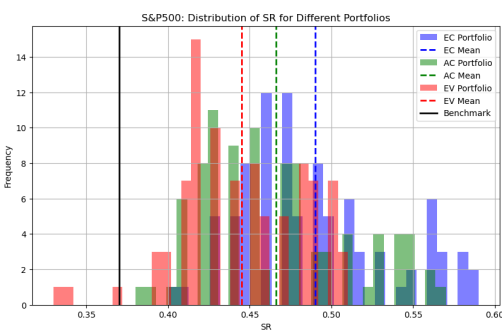


Figure 51: $S\mathcal{E}P500$, $h = 2$: Sharpe Ratio.

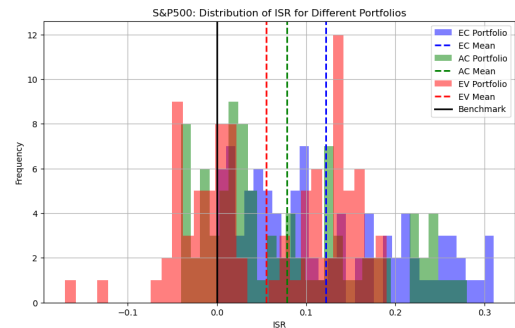


Figure 52: $S\mathcal{E}P500$, $h = 2$: Information Ratio.

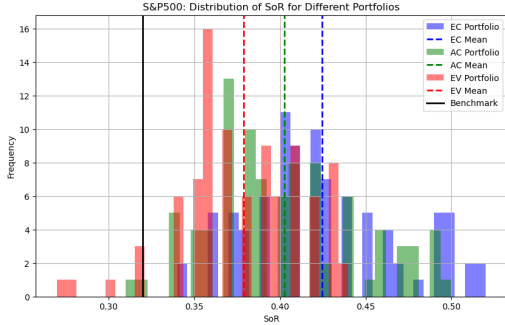


Figure 53: $S\&P500$, $h = 2$: Sortino Ratio.

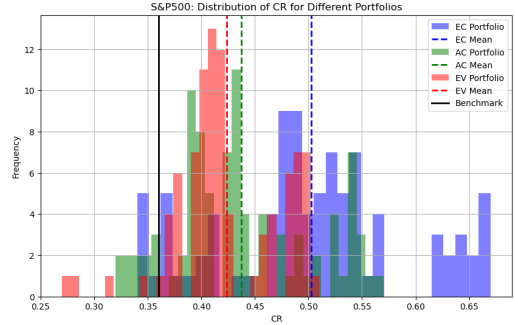


Figure 54: $S\&P500$, $h = 2$: Calmar Ratio.

5.6.2 MSCI World Sectors and MSCI World Index

In this section, we compute again the systemic risk indicators on the 10 GICS sectors of the MSCI World, constructing strategies being the MSCI World index, as done in the corresponding section for the case $h = 1$. The chart 55 shows again the potential of the EC both to control risk and also to enhance returns for the vast majority of adopted thresholds but even in this case, the results are clearly worse with respect to the S&P500 case. The tables 17, 18, 19 and 20 indicate respectively the average and median performance and risk metrics calculated across the bundle of profit and loss curves for each systemic risk indicator.

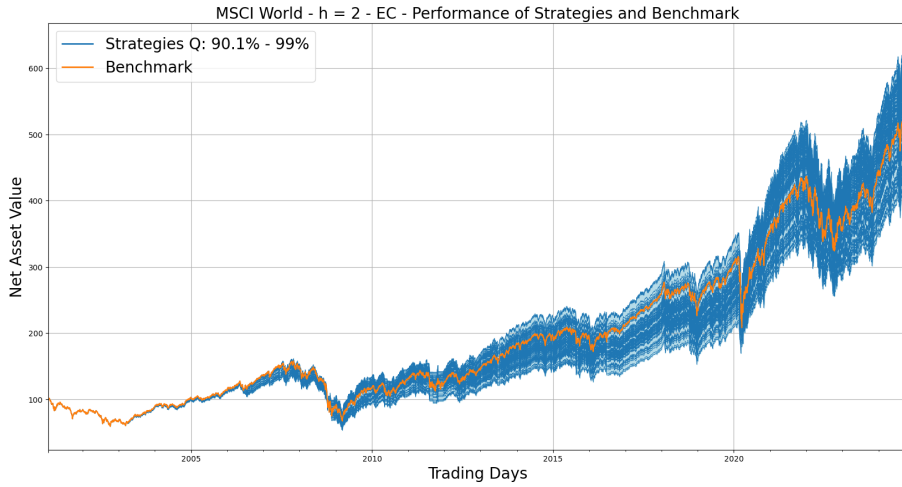


Figure 55: $MSCI$ World, $h = 2$: Profit and Loss curves of strategies based on EC against the Benchmark. The bundle of profit and loss curves of the strategies is obtained by varying the threshold $\bar{\mu}$ along the percentiles from 90% to 99%, in steps of 1%.

Table 17: MSCI World, $h = 2$: Descriptive Statistics of Portfolios (Part 1)

Average	maxD	meanD	VaR	cVaR	mean	std	skew	kurtosis
EC Portfolio	-0.55	-0.106	-0.0142	-0.0224	0.0272	0.913	-0.378	8.83
AC Portfolio	-0.55	-0.106	-0.0142	-0.0224	0.0271	0.914	-0.381	8.89
EV Portfolio	-0.57	-0.115	-0.0143	-0.0228	0.0256	0.921	-0.510	9.42
Benchmark	-0.57	-0.107	-0.0154	-0.0250	0.0271	1.016	-0.600	11.02

 Table 18: MSCI World, $h = 2$: Descriptive Statistics of Portfolios (Part 2)

Average	SR	ISR	SoR	CR
EC Portfolio	0.47	0.005	0.40	0.35
AC Portfolio	0.47	0.002	0.40	0.35
EV Portfolio	0.44	-0.051	0.36	0.32
Benchmark	0.42	NaN	0.36	0.33

As for the maximum drawdown and mean drawdown, both the EC and AC portfolios exhibit on average -0.55 and -0.106, outperforming the EV portfolio and the benchmark, which have both on average maximum drawdown equal to -0.57, and respectively -0.115, -0.107 for the mean drawdown.

The EC and AC portfolios have identical average VaRs of -0.0142 and cVaRs of -0.0224, marginally better than the EV portfolio with a VaR of -0.0143 and cVaR of -0.0228. The benchmark exhibits higher tail risk with a VaR of -0.0154 and a cVaR of -0.0250.

In terms of mean returns, the EC portfolio achieves an average of 0.0272, slightly outperforming both the AC portfolio at 0.0271, and doing better than the EV portfolio at 0.0256. The benchmark's mean return stands at 0.0271, on par with the AC portfolio. The standard deviation is lowest for the EC portfolio at 0.913, followed closely by the AC portfolio. The EV portfolio has a higher volatility of 0.921, while the benchmark exhibits the highest volatility at 1.016.

The EC portfolio attains the highest average SR of 0.47, very close to the AC portfolio and surpassing the EV portfolio at 0.44 and the benchmark at 0.42.

As for the Information Ration, the EC portfolio achieves a result of 0.005, outperforming the AC portfolio at 0.002 and the EV portfolio, which records a negative ISR of -0.051. As for the SoR, the EC achieves again the highest result, but again very close to AC portfolios, clearly outperforming the 0.36 value of both the EV portfolio and the benchmark.

The CR is higher again for the EC and AC portfolios at 0.35, with a slight advantage of the EC one, compared to 0.32 for the EV portfolio and 0.33 for the benchmark.

Skewness and kurtosis metrics reveal the distribution characteristics of the portfolios' returns. The EC portfolio exhibits a skewness of -0.378 and kurtosis of 8.83, indicating a

slight left-skewed distribution with leptokurtic features. The AC portfolio shows similar distributional properties. The EV portfolio has a more pronounced negative skewness of -0.51 and higher kurtosis of 9.42, suggesting greater potential for extreme negative returns. The benchmark has the highest negative skewness at -0.600 and kurtosis at 11.02, highlighting its susceptibility to extreme market movements.

Table 19: MSCI World, $h = 2$: Descriptive Statistics of Portfolios (Part 1)

Median	maxD	meanD	VaR	cVaR	mean	std	skew	kurtosis
EC Portfolio	-0.56	-0.10	-0.014	-0.022	0.0276	0.9028	-0.42	9.36
AC Portfolio	-0.56	-0.10	-0.014	-0.022	0.0276	0.9033	-0.42	9.44
EV Portfolio	-0.58	-0.11	-0.014	-0.023	0.0254	0.9094	-0.45	8.06
Benchmark	-0.57	-0.11	-0.015	-0.025	0.0271	1.0160	-0.60	11.02

Table 20: MSCI World, $h = 2$: Descriptive Statistics of Portfolios (Part 2)

	Median	SR	ISR	SoR	CR
EC Portfolio	0.49	0.02	0.41	0.36	
AC Portfolio	0.48	0.01	0.41	0.36	
EV Portfolio	0.45	-0.05	0.37	0.31	
Benchmark	0.42	NaN	0.36	0.33	

The median metrics fully corroborate the average findings. 57 depicts the distributions of the metrics for the three systemic risk indicators portfolios.

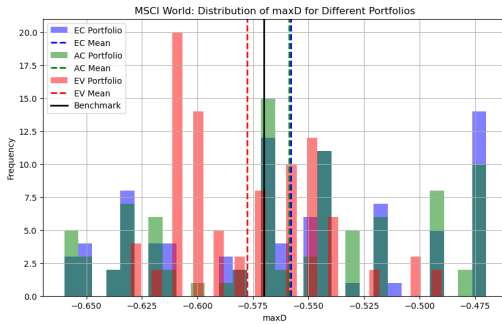


Figure 56: *MSCI World, $h = 2$: Maximum Drawdown Distribution.*

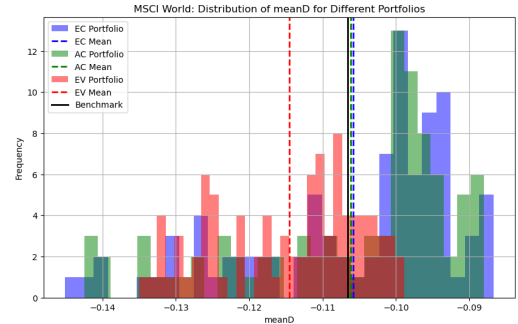


Figure 57: *MSCI World, $h = 2$: Average Drawdown Distribution.*

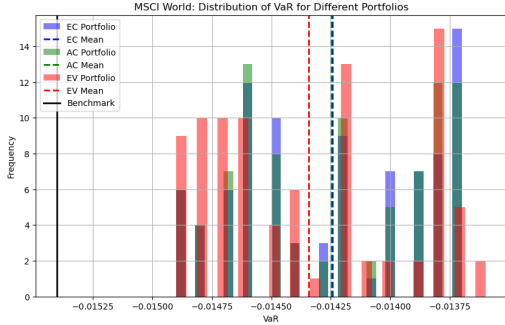


Figure 58: *MSCI World*, $h = 2$: *Value-at-Risk*.

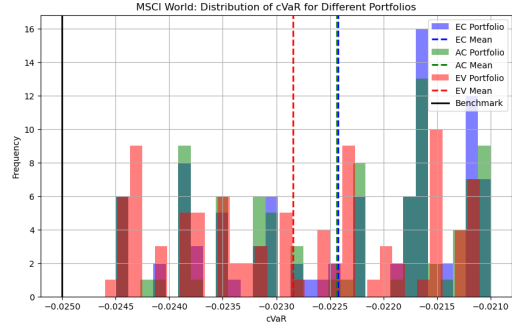


Figure 59: *MSCI World*, $h = 2$: *Conditional Value-at-Risk*.

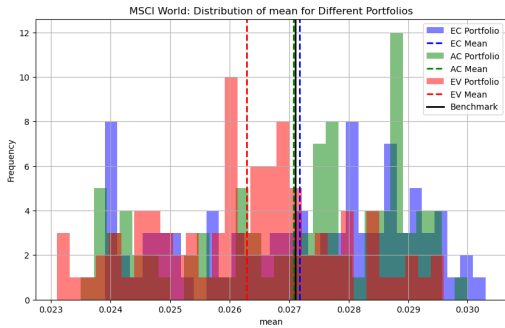


Figure 60: *MSCI World*, $h = 2$: *Returns Mean*.

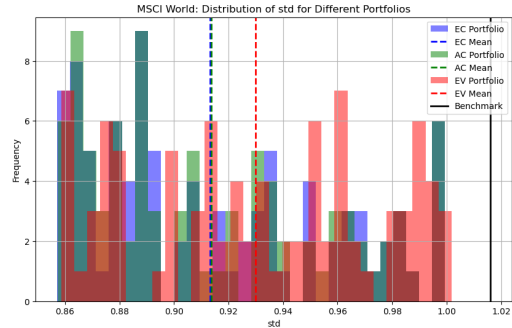


Figure 61: *MSCI World*, $h = 2$: *Returns Standard Deviation*.

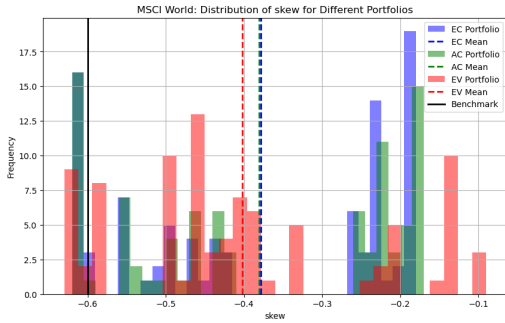


Figure 62: *MSCI World*, $h = 2$: *Returns Skewness*.

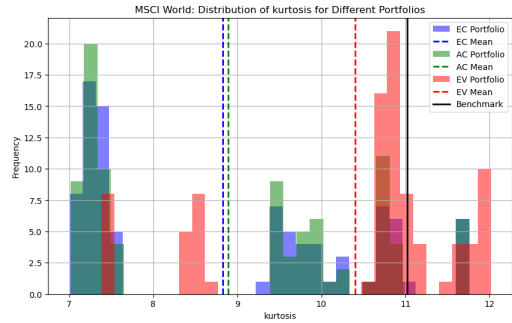


Figure 63: *MSCI World*, $h = 2$: *Returns Kurtosis*.

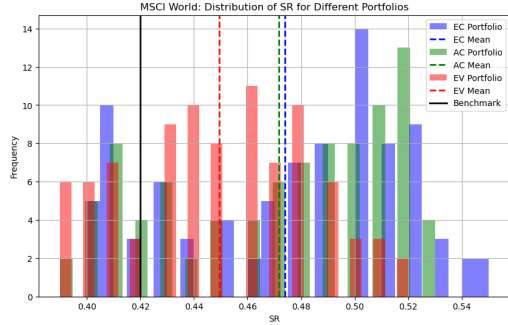


Figure 64: *MSCI World, $h = 2$: Sharpe Ratio.*

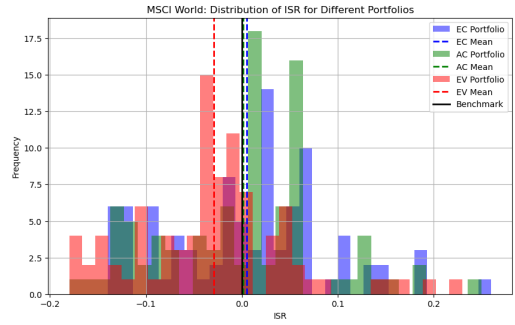


Figure 65: *MSCI World, $h = 2$: Information Ratio.*

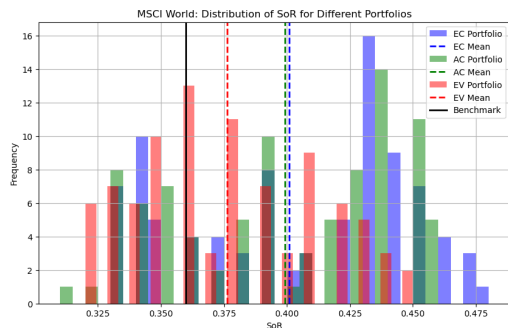


Figure 66: *MSCI World, $h = 2$: Sortino Ratio.*

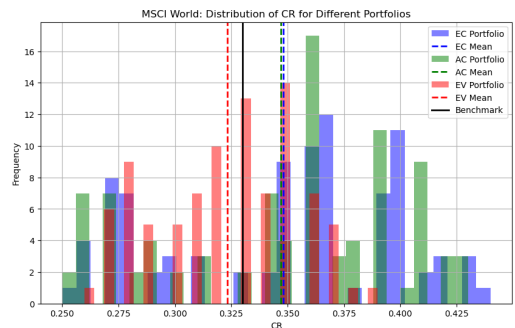


Figure 67: *MSCI World, $h = 2$: Calmar Ratio.*

5.6.3 S&P500 Sectors and MSCI World Index

Even for the case of $h = 2$, it is evident that the indicators have performed better for the S&P500 index compared to the MSCI World index. Therefore and for the same reasons, we replicate the analysis already provided in the corresponding section for the case $h = 1$, that is computing the correlation matrices on the logarithmic returns of the 10 GICS sectors of the S&P500, while applying the indicator-based strategies to the MSCI World index. The chart ?? makes it evident how using the EC on the S&P500 sectors again yields far better results for the prediction of MSCI World index crashes. The tables 21, 22, 23 and 24 show that this result holds also for the AC and EV portfolios.

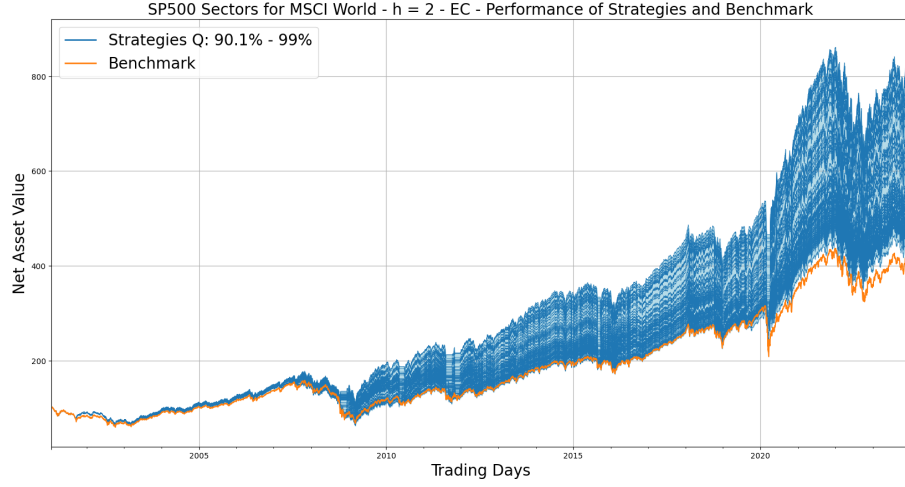


Figure 68: *S&P500 sectors MSCI World, $h = 2$: Profit and Loss curves of strategies based on EC against the Benchmark. The bundle of profit and loss curves of the strategies is obtained by varying the threshold $\bar{\mu}$ along the percentiles from 90% to 99%, in steps of 1%.*

Table 21: S&P500 sectors MSCI World, $h = 2$: Descriptive Statistics of Portfolios (Part 1)

Average	maxD	meanD	VaR	cVaR	mean	std	skew	kurtosis
EC Portfolio	-0.48	-0.083	-0.014	-0.021	0.0302	0.884	-0.27	6.20
AC Portfolio	-0.48	-0.092	-0.014	-0.022	0.0289	0.885	-0.28	6.12
EV Portfolio	-0.49	-0.091	-0.014	-0.022	0.0287	0.897	-0.36	6.98
Benchmark	-0.57	-0.110	-0.016	-0.025	0.0249	1.025	-0.59	10.94

Table 22: S&P500 sectors MSCI World, $h = 2$: Descriptive Statistics of Portfolios (Part 2)

Average	SR	ISR	SoR	CR
EC Portfolio	0.54	0.17	0.48	0.46
AC Portfolio	0.52	0.13	0.46	0.43
EV Portfolio	0.51	0.12	0.44	0.42
Benchmark	0.39	NaN	0.33	0.31

The empirical results indicate that the EC, AC, and EV portfolios consistently outperform the benchmark across key risk and return metrics. Notably, the EC portfolio demonstrates superior performance by achieving higher returns with lower associated risks. Its mean maximum drawdown of -0.482 is significantly less severe than the benchmark's -0.570, highlighting enhanced downside protection. Additionally, the EC portfolio exhibits a lower

average drawdown and reduced volatility, with a standard deviation of 0.884 compared to the benchmark's 1.025, indicating more stable returns.

In terms of return generation, the EC portfolio attains a mean return of 0.0302, outperforming both the AC and EV portfolios, as well as the benchmark at 0.0249. The EC portfolio's favorable balance between return and risk is further emphasized by its superior risk-adjusted performance metrics.

Table 23: S&P500 sectors MSCI World, $h = 2$: Descriptive Statistics of Portfolios (Part 1)

	Median	maxD	meanD	VaR	cVaR	mean	std	skew	kurtosis
EC Portfolio	-0.44	-0.080	-0.014	-0.021	0.0290	0.871	-0.25		5.12
AC Portfolio	-0.45	-0.089	-0.014	-0.021	0.0276	0.873	-0.27	5.09	
EV Portfolio	-0.48	-0.089	-0.014	-0.022	0.0279	0.898	-0.34		6.90
Benchmark	-0.57	-0.110	-0.016	-0.025	0.0249	1.025	-0.59		10.94

Table 24: S&P500 sectors MSCI World, $h = 2$: Descriptive Statistics of Portfolios (Part 2)

	Median	SR	ISR	SoR	CR
EC Portfolio	0.53	0.15	0.48	0.46	
AC Portfolio	0.50	0.10	0.45	0.43	
EV Portfolio	0.51	0.12	0.40	0.42	
Benchmark	0.39	NaN	0.33	0.31	

The Sharpe Ratio for the EC portfolio stands at 0.54, surpassing both the AC portfolio at 0.52, the EV one at 0.51 and the benchmark at 0.39, indicating better compensation for total risk taken. Its Information Ratio of 0.17 reflects strong performance relative to the benchmark, while the Sortino Ratio of 0.48 underscores its efficiency in generating returns adjusted for downside risk. The Calmar Ratio of 0.46 further confirms the EC portfolio's ability to deliver higher returns per unit of maximum drawdown risk, outperforming both competitors and the benchmark. The EC portfolio then clearly outperforms on average all the competing portfolios in terms of all the risk-adjusted performance metrics. The median-based analysis confirms the insights of the average-based one. Analyzing the return distribution characteristics, the EC portfolio exhibits less negative skewness and lower kurtosis compared to the benchmark, as well as with respect to the EV portfolios. This suggests a more favorable distribution with fewer extreme negative returns, enhancing its appeal to investors seeking stable and predictable performance. The median values reinforce these observations, showing consistent superiority of the EC portfolio across

different thresholds.

The graphs provide the metrics distributions across the possible thresholds.

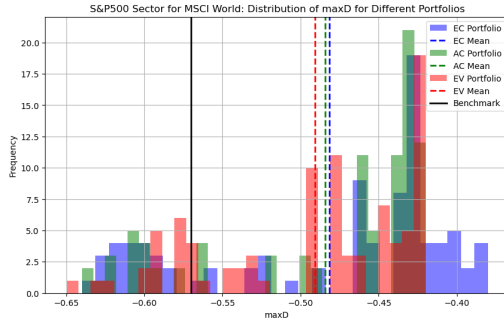


Figure 69: *S&P500 sectors × MSCI World, $h = 2$: Maximum Drawdown Distribution.*

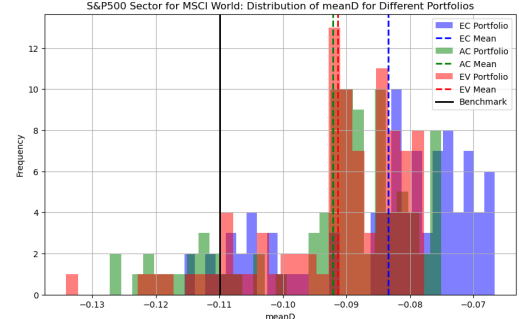


Figure 70: *S&P500 sectors × MSCI World, $h = 2$: Average Drawdown Distribution.*

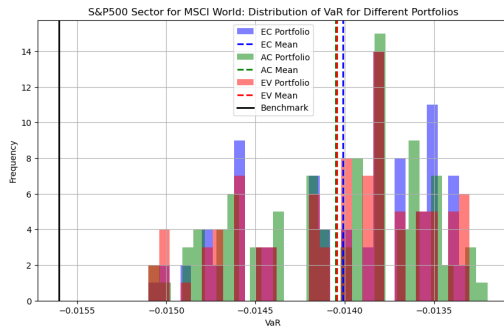


Figure 71: *S&P500 sectors × MSCI World, $h = 2$: Value-at-Risk.*

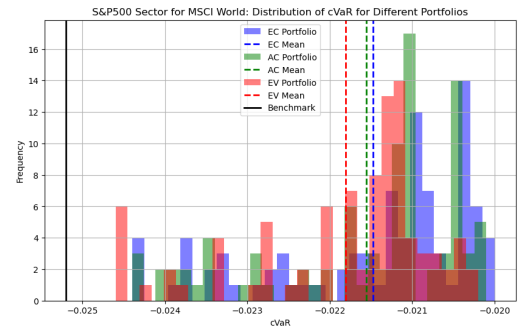


Figure 72: *S&P500 sectors × MSCI World, $h = 2$: Conditional Value-at-Risk.*

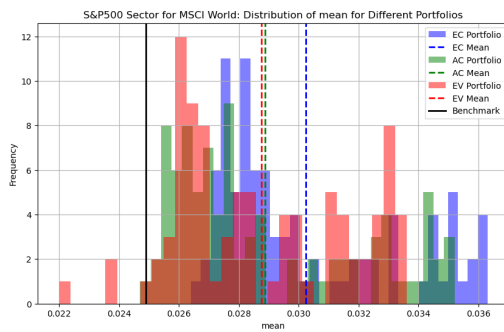


Figure 73: *S&P500 sectors × MSCI World, $h = 2$: Returns Mean.*

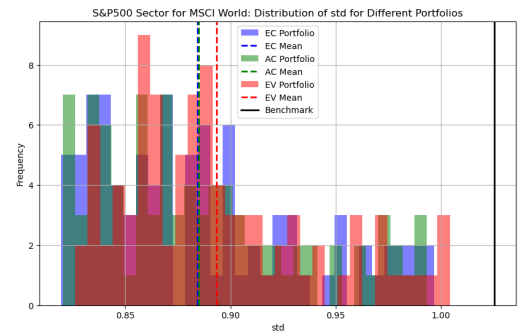


Figure 74: *S&P500 sectors × MSCI World, $h = 2$: Returns Standard Deviation.*

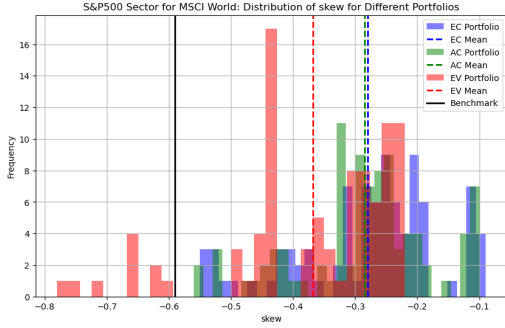


Figure 75: *S&P500 sectors × MSCI World*,
 $h = 2$: Returns Skewness.

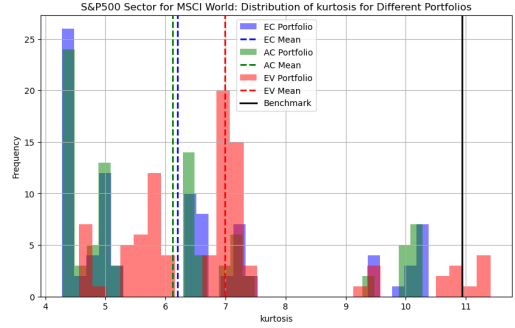


Figure 76: *S&P500 sectors × MSCI World*,
 $h = 2$: Returns Kurtosis.

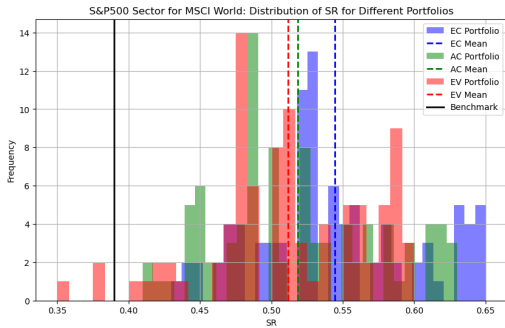


Figure 77: *S&P500 sectors × MSCI World*,
 $h = 2$: Sharpe Ratio.

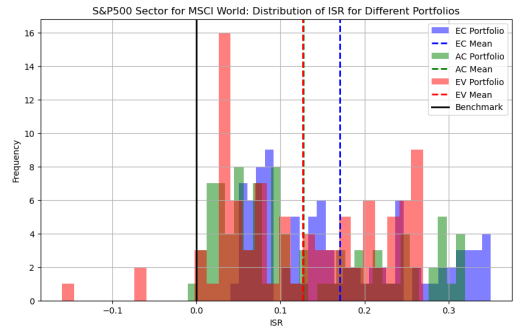


Figure 78: *S&P500 sectors × MSCI World*,
 $h = 2$: Information Ratio.

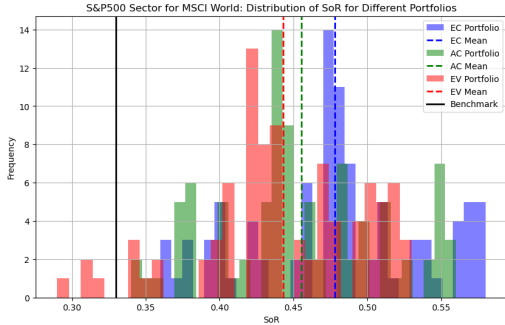


Figure 79: *S&P500 sectors × MSCI World*,
 $h = 2$: Sortino Ratio.

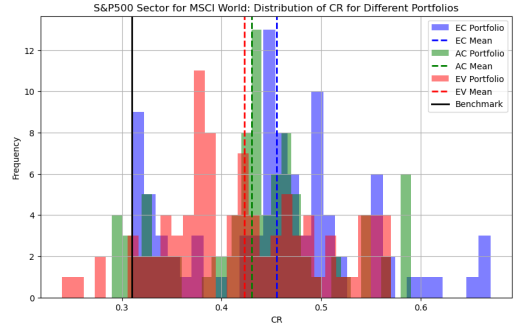


Figure 80: *S&P500 sectors × MSCI World*,
 $h = 2$: Calmar Ratio.

5.7 Performance Analysis of the EC in some systemic stock market crashes

In this section we present the behavior of the EC indicator compared to the benchmark during specific years characterized by significant downturns. In this context, we have selected the 95th percentile of the historical values assumed by the indicator as a reasonable and intermediate threshold. This choice is made for illustrative purposes in relation to

specific stock market crashes.

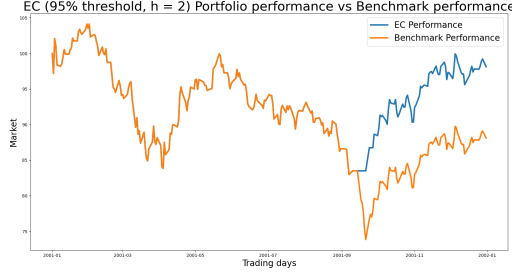


Figure 81: $h = 2$, 2001: EC Portfolio vs Benchmark.

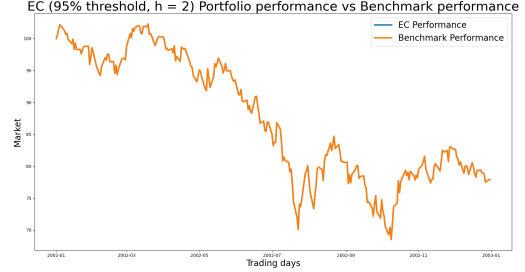


Figure 82: $h = 2$, 2002: EC Portfolio vs Benchmark.

In September 2001 81, the financial markets experienced significant disruption due to the terrorist attacks on September 11. The New York Stock Exchange was closed for four trading sessions and reopened on September 17, 2001. Upon reopening, the S&P 500 fell approximately 11.6% in the week following the attacks, with the aviation, insurance, and tourism industries particularly hard hit. The U.S. government responded with a series of measures to stabilize the economy, including monetary easing by the Federal Reserve, which cut interest rates multiple times. Additionally, significant fiscal stimulus was introduced, including emergency spending and tax cuts, helping to restore investor confidence and stabilize the markets. The EC indicator appears to predict the imminent market crash with remarkable timing 81, 25, 26. However, this is impossible given that such events are entirely unpredictable. More likely, the model has captured some dynamics related to the still unresolved issue of the dot-com bubble—which persisted until 2002—and an already unfavorable market situation.

Table 25: 2001: Descriptive Statistics of Portfolios (Part 1)

	maxD	meanD	VaR	cVaR	mean	std	skew	kurtosis
EC Portfolio	-0.20	-0.0983	-0.0191	-0.0265	-0.0073	1.2611	0.23	1.60
Benchmark	-0.29	-0.1248	-0.0201	-0.0297	-0.0487	1.3259	0.02	1.71

Table 26: 2001: Descriptive Statistics of Portfolios (Part 2)

	SR	ISR	SoR	CR
EC Portfolio	-0.09	1.6	-0.21	-0.25
Benchmark	-0.58	NaN	-1.25	-1.18

Continuing into 2002, the collapse of the dot-com bubble, which began in 2000, led to further economic challenges. Overvalued technology stocks continued to plummet, resulting

in widespread losses. This period was further marred by corporate scandals such as Enron and WorldCom, which were involved in massive accounting fraud, further eroding investor confidence. In response to these crises, regulatory reforms were implemented, including the Sarbanes-Oxley Act of 2002, aimed at improving corporate governance and restoring investor trust. The Federal Reserve's continued cuts in interest rates eventually helped to stabilize the economy and the financial markets. Regarding the 2002 crisis, the model does not provide any signal to deactivate the investment.

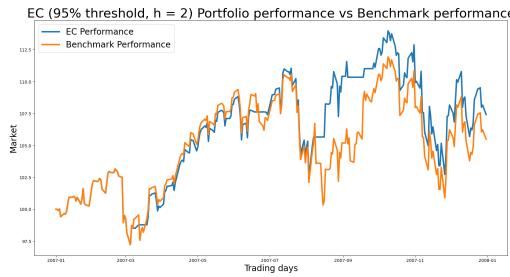


Figure 83: $h = 2$, 2007: EC Portfolio vs Benchmark.

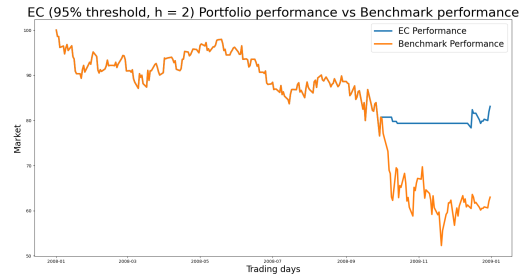


Figure 84: $h = 2$, 2008: EC Portfolio vs Benchmark.

In the second half of 2007, the subprime mortgage crisis began to unfold as financial institutions reported significant losses on mortgage-backed securities, leading to a credit crunch. Rising default rates on subprime mortgages caused widespread panic in the financial markets. In response, the Federal Reserve intervened by cutting interest rates and providing liquidity to financial institutions. The government introduced measures such as the Economic Stimulus Act of 2008 to support the economy. However, these actions were not sufficient to prevent the crisis from escalating. In this case the model enhanced the investment return just by a narrow margin, but it effectively controlled part of the volatility and drawdowns, [83](#) [27](#), [28](#).

Table 27: 2007: Descriptive Statistics of Portfolios (Part 1)

	maxD	meanD	VaR	cVaR	mean	std	skew	kurtosis
EC Portfolio	-0.20	-0.0983	-0.0191	-0.0265	-0.0073	1.2611	0.23	1.60
Benchmark	-0.29	-0.1248	-0.0201	-0.0297	-0.0487	1.3259	0.02	1.71

Table 28: 2007: Descriptive Statistics of Portfolios (Part 2)

	SR	ISR	SoR	CR
EC Portfolio	-0.09	1.6	-0.21	-0.25
Benchmark	-0.58	NaN	-1.25	-1.18

By 2008, the financial crisis had reached its peak, notably marked by the collapse of Lehman Brothers in September. This event triggered severe disruptions in global financial markets, with the S&P 500 losing about 38.5% of its value by the end of the year. The crisis was characterized by the failure of major financial institutions, a severe credit crunch, and a significant decline in consumer wealth. In response, the U.S. government implemented the Troubled Asset Relief Program (TARP), which provided bailout funds to banks and other financial institutions. The Federal Reserve also cut interest rates to near zero and introduced unconventional monetary policy measures such as quantitative easing. These actions helped stabilize the financial system and restore confidence in the markets, with the crisis officially ending as economic recovery began in mid-2009. In this case, the timing of the EC signal was nearly perfect 84, 29, 30.

Table 29: 2008: Descriptive Statistics of Portfolios (Part 1)

	maxD	meanD	VaR	cVaR	mean	std	skew	kurtosis
EC Portfolio	-0.23	-0.1187	-0.0246	-0.0379	-0.0709	1.5051	-0.65	6.48
Benchmark	-0.48	-0.1603	-0.0424	-0.0667	-0.1770	2.5434	-0.04	3.98

Table 30: 2008: Descriptive Statistics of Portfolios (Part 2)

	SR	ISR	SoR	CR
EC Portfolio	-0.75	0.82	-1.43	-2.14
Benchmark	-1.11	NaN	-2.34	-2.62

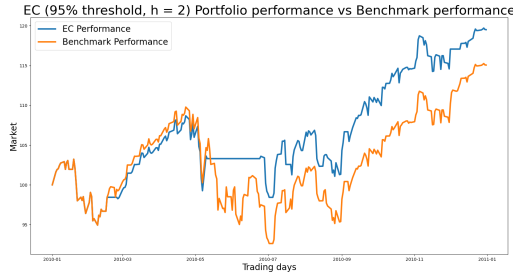


Figure 85: $h = 2$, 2010: EC Portfolio vs Benchmark.

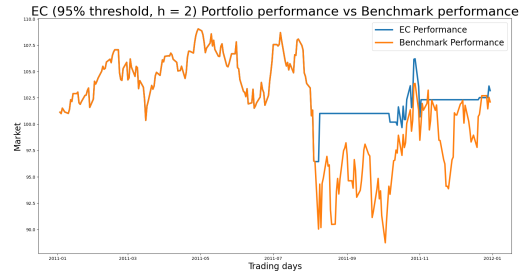


Figure 86: $h = 2$, 2011: EC Portfolio vs Benchmark.

On May 6, 2010, the U.S. stock market experienced the "Flash Crash" during which the Dow Jones Industrial Average dropped nearly 1,000 points within minutes before recovering. Simultaneously, concerns over the European Sovereign Debt Crisis, particularly in Greece, led to fears of potential default and market instability. In response to the Flash Crash, U.S. regulators implemented new rules to improve market stability, including circuit breakers designed to prevent similar events. The European Union and International

Monetary Fund provided bailout packages to Greece and other affected countries, while the European Central Bank introduced measures to support the eurozone economy. The EC improved by a non-negligible margin the performance, as well as the risk control 85, 31, 32.

Table 31: 2010: Descriptive Statistics of Portfolios (Part 1)

	maxD	meanD	VaR	cVaR	mean	std	skew	kurtosis
EC Portfolio	-0.09	-0.0270	-0.0155	-0.0237	0.0686	0.9389	-0.12	3.77
Benchmark	-0.16	-0.0494	-0.0171	-0.0272	0.0540	1.1205	-0.21	2.18

Table 32: 2010: Descriptive Statistics of Portfolios (Part 2)

	SR	ISR	SoR	CR
EC Portfolio	1.16	0.38	2.35	5.13
Benchmark	0.77	NaN	1.72	2.44

From July to October 2011, the U.S. faced the debt ceiling crisis, leading to fears of a potential government default and significant market volatility. The situation was further exacerbated in August 2011 when Standard & Poor's downgraded the U.S. credit rating. Concurrently, the European debt crisis continued to weigh on investor sentiment, with countries like Greece, Italy, and Spain facing severe fiscal challenges. To address these issues, the U.S. Congress reached a last-minute agreement to raise the debt ceiling, thereby averting a default. The European Central Bank and other international organizations continued to provide support to struggling eurozone countries through additional bailout packages and monetary easing measures. These actions helped stabilize the markets over time. In this case the indicator improved the performance just by a negligible margin, showing some delay in market entrance and then losing part of the rally, but it clearly reduced drawdowns and downside volatility 86, 33, 34.

Table 33: 2011: Descriptive Statistics of Portfolios (Part 1)

Average	maxD	meanD	VaR	cVaR	mean	std	skew	kurtosis
EC Portfolio	-0.12	-0.0407	-0.0176	-0.0236	0.0078	0.8911	-0.36	7.12
Benchmark	-0.19	-0.0565	-0.0251	-0.0360	0.0037	1.4503	-0.52	3.10

Table 34: 2011: Descriptive Statistics of Portfolios (Part 2)

	SR	ISR	SoR	CR
EC Portfolio	0.14	0.06	0.26	0.47
Benchmark	0.04	NaN	0.09	0.14



Figure 87: $h = 2$, 2015: EC Portfolio vs Benchmark.

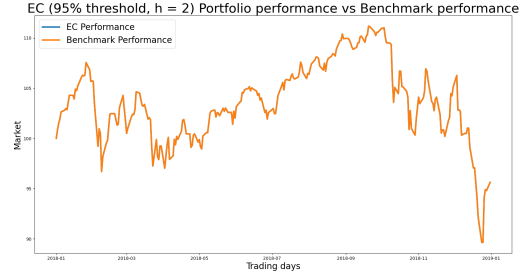


Figure 88: $h = 2$, 2018: EC Portfolio vs Benchmark.

In August 2015, the Chinese stock market experienced significant volatility, sending shockwaves through global markets. Concerns over China's economic slowdown and a surprise devaluation of the yuan contributed to fears of a global economic downturn, leading to significant declines in the S&P 500. To stabilize the stock market, the Chinese government intervened with several measures, including halting trading on certain stocks, restricting short-selling, and injecting liquidity into the market. Additionally, the People's Bank of China cut interest rates and reduced reserve requirements for banks. These actions helped to calm the markets. As for this crash, the indicator's contribution was positive but modest both in performance and in risk sides 87, 35, 36.

Table 35: 2015: Descriptive Statistics of Portfolios (Part 1)

	maxD	meanD	VaR	cVaR	mean	std	skew	kurtosis
EC Portfolio	-0.12	-0.0218	-0.0142	-0.0211	0.0087	0.9005	-0.22	2.77
Benchmark	-0.12	-0.0241	-0.0150	-0.0224	0.0053	0.9617	-0.23	2.12

Table 36: 2015: Descriptive Statistics of Portfolios (Part 2)

	SR	ISR	SoR	CR
EC Portfolio	0.15	0.16	0.30	0.51
Benchmark	0.09	NaN	0.18	0.31

In late 2018, the U.S. stock market experienced significant volatility, culminating in a sharp

decline in the S&P 500. From its peak in late September to its trough in late December, the S&P 500 fell nearly 20%, marking it as the worst December performance since the Great Depression. Several factors contributed to this crash, including concerns over rising interest rates, trade tensions between the U.S. and China, and fears of a global economic slowdown. The Federal Reserve's decision to continue raising interest rates despite market apprehensions added to the negative sentiment. In response to the market turmoil, the Federal Reserve signaled a more dovish stance in early 2019, indicating a pause in interest rate hikes. This shift in monetary policy helped to calm investor fears and contributed to a market rebound. Additionally, progress in trade negotiations between the U.S. and China helped to alleviate some of the uncertainties. These measures, combined with strong corporate earnings reports, led to a recovery in the stock markets, with the S&P 500 regaining much of its lost ground by the first quarter of 2019. In this case the EC failed in spotting the danger [88](#).

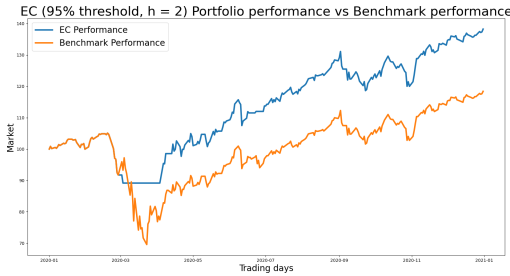


Figure 89: $h = 2$, 2020: EC Portfolio vs Benchmark.

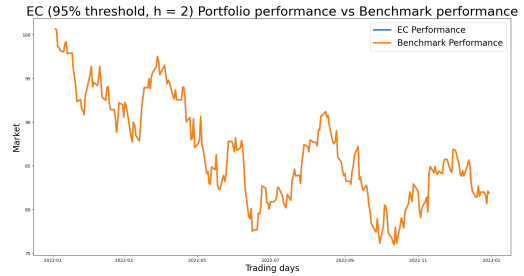


Figure 90: $h = 2$, 2020: EC Portfolio vs Benchmark.

In 2020, the outbreak of the COVID-19 pandemic led to unprecedented global economic disruptions. In March 2020, the S&P 500 fell nearly 34% from its peak in February to its trough, marking one of the fastest market declines in history. Lockdowns, business closures, and widespread uncertainty contributed to the market turmoil. Governments and central banks around the world responded with massive fiscal and monetary stimulus measures. In the U.S., the Federal Reserve cut interest rates to near zero and introduced extensive quantitative easing programs. The government passed several stimulus packages, including direct payments to individuals, enhanced unemployment benefits, and support for businesses. These measures helped to stabilize the economy and led to a rapid recovery in the stock markets. In this case, the EC signals was close to perfection in terms of both sides of timing: exit and entry signals [89](#), [37](#), [38](#).

Table 37: 2020: Descriptive Statistics of Portfolios (Part 1)

	maxD	meanD	VaR	cVaR	mean	std	skew	kurtosis
EC Portfolio	-0.15	-0.0343	-0.0188	-0.0327	0.1241	1.2604	-0.37	5.80
Benchmark	-0.34	-0.0672	-0.0340	-0.0573	0.0647	2.1512	-0.88	9.06

Table 38: 2020: Descriptive Statistics of Portfolios (Part 2)

	SR	ISR	SoR	CR
EC Portfolio	1.57	0.54	3.02	5.78
Benchmark	0.48	NaN	0.87	1.35

In 2022, concerns over rising inflation, potential interest rate hikes by the Federal Reserve, and geopolitical tensions, such as the Russia-Ukraine conflict, led to significant market volatility. Supply chain disruptions and labor shortages contributed to inflationary pressures, while geopolitical risks heightened uncertainty. The Federal Reserve began to signal a more aggressive stance on monetary policy, including potential interest rate hikes to combat inflation. Additionally, diplomatic efforts were made to address geopolitical tensions, although these remained ongoing. Market participants adjusted their expectations, leading to periods of stabilization. In this case the indicator failed, not producing any kind of signal 90.

6 Conclusion

In this study, we introduce a class of connectivity measures based on the general definition of entropy provided by Rényi, demonstrating that they are proper connectivity measures. The properties of these measures coherently integrate two different perspectives proposed in the literature, which respectively focused on the highest eigenvalue of covariance or correlation matrices or the lowest eigenvalues. Additionally, while existing models attempting to unify these two perspectives required the calibration of additional hyperparameters related to the number of minor eigenvalues to consider, the connectivity measures based on Rényi entropy proposed here overcome this issue by considering all of them.

In the empirical section, using sector returns and simulating trading strategies on the S&P 500 and MSCI World indices over two different time horizons, we demonstrate the predictive power of the connectivity indicators introduced in this work. A comparison with similar measures revealed that, despite slight fluctuations in results depending on the dataset and forecast horizon considered, the indicator proposed in this study tends to consistently provide more effective signals.

References

- [1] Acemoglu, D., Ozdaglar, A., & Tahbaz-Salehi, A. (2015). Systemic Risk and Stability in Financial Networks. *American Economic Review*, 105(2), 564-608.
- [2] Acharya, V. V., Engle, R., & Richardson, M. (2012). Capital shortfall: A new approach to ranking and regulating systemic risks. *American Economic Review*, 102, 59-64.
- [3] Alessi, L., & Detken, C. (2011). Quasi real time early warning indicators for financial crises. *International Journal of Forecasting*, 27(3), 832-844.
- [4] Andersen, T. G., Bollerslev, T., & Diebold, F. X. (2010). Parametric and nonparametric volatility measurement. In *Handbook of Financial Econometrics: Tools and Techniques*, Handbook in Finance 1, 67-137.
- [5] Barunik, J., Kocenda, E., & Vacha, L. (2016). Asymmetric connectedness on the U.S. stock market: Bad and good volatility spillovers. *Journal of Financial Markets*, 27, 55-78.
- [6] Belsley, D. A., Kuh, E., & Welsch, R. R. (1980). *Regression Diagnostics: Identifying Influential Data and Sources of Collinearity*. New York: John Wiley Sons.
- [7] Bilson, J. F. O. (1979). Leading indicators of currency devaluations. *Columbia Journal of World Business*, 14, 62-76.
- [8] Billio, M., Getmansky, M., Lo, A. W., & Pelizzon, L. (2012). Econometric measure of connectedness and systemic risk in the finance and insurance sectors. *Journal of Financial Economics*, 104(3), 535-559.
- [9] Caraiani, P. (2014). The predictive power of singular value decomposition entropy for stock market dynamics. *Physica A: Statistical Mechanics and its Applications*, 393, 571-578.
- [10] Caraiani, P. (2018). Modeling the comovement of entropy between financial markets. *Entropy*, 20(6), 417.
- [11] Civitarese, J. (2016). Volatility and correlation-based systemic risk measures in the US market. *Physica A: Statistical Mechanics and its Applications*, 459, 55-67.
- [12] Cover, T. M., & Thomas, J. A. (2006). *Elements of Information Theory* (2nd ed.). Wiley-Interscience.
- [13] Demirer, M., Diebold, F. X., Liu, L., & Yilmaz, K. (2018). Estimating global bank network connectedness. *Journal of Applied Econometrics*, 33(1), 1-15.

- [14] Diebold, F. X., & Yilmaz, K. (2009). Measuring financial asset return and volatility spillovers, with application to global equity markets. *Economic Journal*, 119, 158-171.
- [15] Diebold, F. X., & Yilmaz, K. (2014). On the network topology of variance decompositions: Measuring the connectedness of financial firms. *Journal of Econometrics*, 182, 119-134.
- [16] Espinosa-Paredes, G., Rodriguez, E., & Alvarez-Ramirez, J. (2022). A singular value decomposition entropy approach to assess the impact of Covid-19 on the informational efficiency of the WTI crude oil market. *Chaos Solitons Fractals*, 160, 112238.
- [17] Figini, S., Maggi, M., & Uberti, P. (2018). The market rank indicator to detect financial distress. *Econometrics and Statistics*, in press.
- [18] Frankel, J. A., & Saravelos, G. (2010). Are Leading Indicators Of Financial Crises Useful For Assessing Country Vulnerability? Evidence From The 2008-09 Global Crisis. *National Bureau of Economic Research Working Paper*, No. 16047.
- [19] Goldenfeld, N. (1992). *Lectures on phase transitions and the renormalization group*. Reading: Addison-Wesley Publishing Company.
- [20] Gu, R. (2017). Multiscale Shannon entropy and its application in the stock market. *Physica A: Statistical Mechanics and its Applications*, 484, 215-224.
- [21] Johansen, A., Ledoit, O., Sornette, D. (2000). Crashes as critical points. *International Journal of Theoretical and Applied Finance*, 3(2), 219-255.
- [22] Kaminsky, G. L. (1999). Currency and Banking Crises: The Early Warnings of Distress. *International Monetary Fund Working Paper*, 99/178.
- [23] Koushki, A., Osoolian, M., & Sadeghi Sharif, S. J. (2023). An uncertainty measure based on Pearson correlation as well as a multiscale generalized Shannon-based entropy with financial market applications. *International Journal of Nonlinear Sciences and Numerical Simulation*, 24(5), 1821-1839.
- [24] Krugman, P. (1979). A model of balance-of-payments crises. *Journal of Money, Credit and Banking*, 11(3), 311-325.
- [25] Lupu, R., et al. (2020). A Bayesian entropy approach to sectoral systemic risk modeling. *Entropy*, 22(12), 1371.
- [26] Lupu, R., et al. (2022). Entropy as Leading Indicator for Extreme Systemic Risk Events. *Romanian Journal of Economic Forecasting*, 25(4), 58.
- [27] Maggi, M., Torrente, M. L., & Uberti, P. (2020). Proper measures of connectedness. *Annals of Finance*, 16(4), 547-571.

- [28] Merton, R. C. (2014). Measuring the Connectedness of the Financial System: Implications for Risk Management. *E-Q Research Bulletin*, 5(1), 1-15.
- [29] Müller-Lennert, M., Dupuis, F., Szehr, O., Fehr, S., & Tomamichel, M. (2013). On Quantum Rényi Entropies: A New Generalization and Some Properties. *Journal of Mathematical Physics*, 54(12), 122203.
- [30] Qyrana, M., Carrara, C., & Figini, S. (2024). Market Stress Detection Through Autoencoder's Deep Latent Factors and Random Matrix Theory. Available at SSRN 4930925
- [31] Rényi, A. (1961). On Measures of Entropy and Information. In *Proceedings of the Fourth Berkeley Symposium on Mathematical Statistics and Probability*, Vol. 1 (pp. 547–561). University of California Press.
- [32] Rose, A. K., & Spiegel, M. M. (2012). Cross-border financial spillovers and systemic risk. *University of California Press*.
- [33] Sornette, D., Johansen, A., & Bouchaud, J. P. (1996). Stock market crashes, Precursors and Replicas. *Journal de Physique I*, 6, 167-175.
- [34] Sornette, D., & Johansen, A. (1997). Large financial crashes. *Physica A*, 245, 411-422.
- [35] Van Erven, T., & Harremoës, P. (2014). Rényi Divergence and Kullback-Leibler Divergence. *IEEE Transactions on Information Theory*, 60(7), 3797–3820.
- [36] Zhang, Y., & Broadstock, D. C. (2018). Global financial connectedness and systemic risk. *Journal of International Financial Markets, Institutions and Money*, 56, 1-22.